NPL Report CIRM 19
September 1998

NATIONAL PHYSICAL LABORATORY

Re-calibration and Monte Carlo Modelling of the NPL Long Counters

Hamid Tagziria and David J Thomas

CIRM, National Physical Laboratory, Teddington, Middlesex, TW11 0LW, UK

Abstract

The Monte Carlo technique has become a very powerful tool in radiation transport as full advantage is taken of richer cross section data, more powerful computers and Monte Carlo techniques, high quality physics, and better known neutron and photon source spectra. At the National Physical Laboratory calculations using the Monte Carlo radiation transport code MCNP have been combined with accurate measurements to characterise two long counters routinely used to standardise monoenergetic neutron fields. New and more accurate response function curves have been produced for both long counters. A novel approach using Monte Carlo methods has been developed, validated and used to model the efficiency of the counters and to determine more accurately their effective centres, which have always been difficult to establish. Calculations and measurements agree well, especially for the De Pangher long counter for which details of the design and constructional material are well known.

ISSN 1369-6793

National Physical Laboratory
Teddington, Middlesex, UK, TW11 0LW

Approved on behalf of Managing Director NPL, by Dr Julian Hunt
Head, Centre for Ionising Radiation Metrology.

TABLE OF CONTENTS

1. INTRODUCTION

The search for a neutron detector which is robust, insensitive to γ-rays, reasonably directional, and has an efficiency that is high and roughly independent of the energy of the incident neutrons culminated in the development of the most popular of all flat response detectors, the **long counter**. Its principle is based on the use of a slow neutron detector within a carefully designed moderating medium. It was Hanson and McKibben[1] who first suggested in 1947 the combination of a boron trifluoride (BF_3) proportional counter tube, from which the long counter draws most of its characteristics, with a cylindrical paraffin moderator, surrounded by an outer annulus, also of paraffin, and an intermediate boron oxide (BO_2) annulus. The reaction involved in the BF_3 slow neutron detector is $^{10}B(n,\alpha)^7Li$ which has a large cross section and a 1/v dependence as its main advantages[2]. The outer paraffin annulus and BO_2 layer act as a shield ensuring that neutrons hitting the sides of the long counter have a low probability of being counted. Only those striking the front face have a high probability of reaching the slow neutron detector. Holes, drilled in the front of the moderator, improve the efficiency for counting low energy neutrons, which would otherwise be absorbed before reaching the BF_3 tube, thus further flattening the response function below a few hundred keV. A cadmium sheet was added on the front face of the counter to shield against thermal neutrons. The Hanson design was followed ten years later by an improved version by McTaggart [3] which received widespread acceptance as the standard long counter. However, various measurements using these counters showed that the response was not reproducible from counter to counter. In 1966, De Pangher and Nichols [4], with reproducibility in mind, improved on the design (Figure 1.1) mainly by specifying the internal and external dimensions of the counter and by using high density polyethylene as the moderator, boron loaded polyethylene for the inner layer of the shield, an aluminium outer casing, and thicker cadmium sheets both at the front and back of the counters. They also replaced the front holes by an annular trough. A batch of six of these counters, known as De Pangher counters, were produced in the UK, and an inter-comparison reported by Marshall [5] showed good agreement (within 0.5%) for their efficiency when measuring neutrons from two radioactive sources with widely different neutron spectral characteristics.

The National Physical Laboratory has two types of long counters. One type is the De Pangher long counter (Figure 1.2) with a 38 mm (1½") outer diameter BF_3 tube, and it is one of the six mentioned above. The other, built at NPL, is a McTaggart type (Figure 1.3) which has a 50 mm (2") outer diameter BF_3 tube for increased efficiency. These counters will be referred to as the De Pangher long counter and the NPL long counter respectively.

At the NPL, neutron fluences are standardised using the above long counters, and since they are neither 100% efficient nor perfectly flat in their response as a function of neutron energy, they themselves need to be calibrated. The solution adopted in this work was to:

1) measure the response with well characterised radioactive neutron sources,
2) predict the response functions by Monte Carlo radiation transport calculations,
3) normalise the predicted response curves using the source measurements.

The counters were last calibrated in the late 1970's and early 1980's by Hunt [6] using a similar method to the above. However, the responses functions were then calculated empirically, using a formula based on available hydrogen and carbon cross section data (BNL325), as suggested by Allen [7]. Although regular source checks have shown that the counters have been extremely stable over the last 20 years (Figure 1.4), it was decided that the counters were due for a re-calibration, for three main reasons:

1) The spectra of radionuclide neutron sources are now better known. There have been improvements in the techniques used to measure source emission rates, and source emission anisotropy factors are better known.

2) The cross section data libraries (ENDF/B-VI, ENDL, JEFF etc.) are richer, in that they are more extensive, and have also been better evaluated and validated.

3) The Monte Carlo method in particle transport calculations has become a very attractive tool because of: advances in computers, the access to modern cross section data libraries, and high quality physics in both the cross section data and the radiation transport codes. The response functions can thus be more accurately simulated than those previously predicted empirically. (Measurements are not always possible, or for some users not affordable, especially at some neutron energies.)

Over the years, it has been widespread practice to assume that the response function, or simply the efficiency, of the long counter is constant with energy. It will be shown in this work that this is far from being the case as significant variations and narrow structures are revealed from 1 keV up to 20 MeV. The limitations of the empirical predictions, the adjustments of the response function as well as the improvements to the cross section data used since the 1970's, will also be shown.

When making measurements of fluence from a point source, the long counter can, provided the source to detector distance is reasonably large ($\geq$ 1 m), be regarded as a point detector. The position of this point, commonly called the effective centre, depends on the design of the counter and the neutron energy, and must be accurately known for any fluence measurement. The determination of the counter effective centre with a reasonable accuracy and reproducibility has represented a serious challenge to calibrating laboratories and users alike. Results often conflicted, were widely spread, and depended on many parameters such as the person making the measurements, scatter corrections methodology, the room size, etc. In this work, a good deal of effort has been expanded in this area and, although work is still progressing at the time of writing this report, a new and promising approach has been developed, the preliminary results of which are reported.

In the following sections, the most extensive re-calibration and Monte Carlo modelling ever undertaken for the long counters since their development are reported. The power of combining good measurements with sound Monte Carlo simulations based on good cross section data and good physics, naturally stands out.

2. MEASUREMENTS

2.1 Experimental Set-up

Both the De Pangher and NPL long counters were re-calibrated, in terms of the variation of both their efficiency and effective centre as a function of neutron energy using radioactive neutron sources, and in terms of their effective centre using monoenergetic neutrons produced by the NPL 3.5 MV Van de Graaff accelerator. Measurements were carried out over many weeks, in a large low-scatter cell at more than 30 source-to-counter distances ranging from 1.2 m to 5 m, from which the efficiency and the effective centre of the counters were evaluated. With either a radionuclide source or the neutron producing target fixed in place at the centre of the cell, the counter's position was varied in 5 to 20 cm steps, and the integrated counts were recorded at each of the 30 or more counter positions. The counter sits on an automatically controlled carriage and can be remotely moved toward or away from the source.

The low scatter cell at NPL is approximately 25 m long by 18 m wide surrounded by concrete walls which are 1 m thick in most places. The roof, made of about 15 cm thick concrete, is 12 meters above the target position which itself is 6 m above a concrete floor. The shadow cone technique [6, 8-10] was used to correct for the scattering of neutrons by the air, the walls, the floors, and the ceiling of the room. This technique involves making measurements with, and without, a shadow cone (Figure 2.1) positioned between the source and the counter. The shadow cone is made of a 20 cm long iron cone in its front part, i.e., the part closest to the source of neutrons, while its rear section, 20 or 30 cm in length, is a hollow truncated cone, filled with a mixture of paraffin wax (50%), polyethylene (10%) and boron oxide powder (40%) produced by melting the three components together and pouring them into the cone. A full discussion of the shadow cone technique, and many other experimental and data analysis matters related to this work, can be found in references 5 and 9 and so will not be detailed here. The experimental set-up is shown in Figure 2.2. The dead time of the counting system was fixed to 10 μs. A correctly chosen shadow cone was positioned at the optimum distance from the source; the choices, which are easily and consistently made using a computer programme, depend on the detector-to-source distance and on the size of both the counter and the source in use. A separate investigation, not covered in this work, has shown that the choices of shadow cones and cone-to source distances were well founded.

2.2 Efficiency and Effective Centre Measurements with Neutron Sources

Five radionuclide neutron sources (^{238}Pu-Li, ^{241}Am-F, ^{252}Cf, ^{241}Am-B and ^{241}Am-Be), three of which are recommended by the International Organization for Standardization, ISO[11], have been used. Details of the encapsulation, source strength and anisotropy [12] are given in Table 2.1, together with some details of the shadow cones used and the optimum shadow cone to source distance.

Table 2.1: Details of radionuclide neutron sources used

	Serial number	Capsule type	Cone numbers	Distance (cm)	Mean Energy (MeV)	Emission rate (s^{-1})	Anisotropy factor
De Pangher long counter							
^{252}Cf	4774NC	X35	8,1	9	2.20	7.67×10^7	1.0207 ± 0.0007
Am-Be	1000/1095	X3	8,1	9	4.30	2.44×10^6	1.0276 ± 0.0025
Pu-Li	MRC-PuLi-63		7	6	0.53	8.47×10^5	1.0777 ± 0.0020
Am-F	1000/7582F	X3	8,1	9	1.46	1.36×10^5	1.0224 ± 0.0007
NPL long counter							
^{252}Cf	4774NC	X35	8,1	9	2.20	8.96×10^7	1.0207 ± 0.0007
Am-Be	1000/1095	X3	8,1	9	4.30	2.44×10^6	1.0276 ± 0.0025
Am-B	1000/7584B	X3	8,1	9	2.72	4.38×10^5	1.0345 ± 0.0026
Pu-Li	MRC-PuLi-63		7	6	0.53	8.43×10^5	1.0777 ± 0.0020
Am-F	1000/7582F	X3	8,1	9	1.46	1.36×10^5	1.0224 ± 0.0007

For all sources, except the ^{238}Pu-Li source, the shadow cone numbered 8 (1), positioned at 9 cm from the source vertical axis, was used for source to counter distances below (above) 250 cm, respectively. The shadow cone numbered 7 was positioned 6 cm from the source for measurement with the ^{238}Pu-Li source. Figure 2.3 shows, for the ^{252}Cf source; the inverse of the square root of the direct counts measured by the NPL long counter, after correction for dead time and in-scatter, versus the source to counter distance. Similar curves were produced for all sources used and for both long counters. They provide a good check on the measurements and analysis of the data in general and on the shadow cone correction in particular.

2.3 Effective Centre Measurements using Monoenergetic Neutrons

The Van de Graaff accelerator was used to produce monoenergetic neutrons via the ^{7}Li(p,n)^{7}Be, the T(p,n)^{3}He, and D(d,n)^{3}He reactions. Measurements were made at five ISO[11] energies, namely 0.144, 0.565, 1.2, 2.5 and 5 MeV. The shadow cone numbered 8 (1), positioned at 9 (11) cm from the target, was used for target to counter distances below (above) about 250 cm, respectively. Figures 2.4 and 2.5 show, for measurements made at a neutron energies of 565 keV and 1200 keV; the inverse of the square root of the direct counts, after correction for dead time and in-scatter, versus source to counter distance. Similar curves were produced for all other energies and for both long counters.

3. DATA ANALYSIS

For a point detector and a point source in vacuum one can write that:

$$C(r)\, r^2 = \text{Constant}$$

where $C(r)$ is the detector count rate at a source-to-counter distance r

Allowing for scatter and geometry effects, a corresponding expression for a long counter, which is about 50 cm in length and 22 cm in radius, has been suggested by Hunt [6,8,10] and is given by:

$$[C_t(r) - C_i(r)]F_a(r) = \frac{K}{(r + r_o)^2}$$

where

$C_t(r)$ and $C_i(r)$ are total and in-scatter measured count rates at a source to detector distance r measured to the front face of the polyethylene,

$F_a(r)$ is the air out-scatter correction (derived from the oxygen and nitrogen cross sections),

r_0 is the effective centre distance into the moderator front face,

and K is the source-detector characteristic constant.

Rearranging the above expression gives:

$$1\Big/\sqrt{[C_t(r) - C_i(r)]F_a(r)} = \sqrt{\frac{1}{K}}(r + r_o)$$

and it follows that r_0 and K can be obtained by a least squares fit, i.e.

$$1\Big/\sqrt{[C_t(r) - C_i(r)]F_a(r)} \quad \text{against } r$$

with the gradient equal to $\sqrt{\frac{1}{K}}$ and the intercept equal to $\sqrt{\frac{1}{K}}\, r_o$

Subsequently, the efficiency ε can be evaluated from:

$$\varepsilon = \frac{4\pi K}{QF_I} \qquad (4)$$

where Q is the source strength, i.e., the total emission rate into 4π steradians, and F_I is the anisotropy factor of the radionuclide source.

The least square fit analysis may be carried out using either PCINVFIT, a FORTRAN computer programme originally written by Hunt, and now adapted to run on a PC, or using the least-squares fitting function within ORIGIN™, a commercially available graphics and statistical analysis package. Both ORIGIN and PCINVFIT gave the same results. It is important that the correct weights are used for the inverse of the square root of the direct counts. These should be based on the statistical uncertainties in both $C_t(r)$ and $C_i(r)$ and correct error propagation techniques. Use of these weights ensures that χ^2 for each source to counter distance (i.e. weight * (calculated - measured)^2) is approximately equal to unity and that the overall χ^2 is roughly equal to the number of data points. PCINVFIT has a facility whereby data points are successively removed from the set, starting with the closest points, and the gradient and intercept are re-calculated. This process is then repeated starting with the furthest point. The fit is accepted only if both the gradient and intercept were stable under this process, allowing for the gradual increase in the uncertainties as fewer and fewer data points are involved in the fit.

4. RESULTS OF EFFICIENCY AND EFFECTIVE CENTRE MEASUREMENTS

4.1 The De Pangher Long Counter

Data obtained with the shadow cone method were analysed as outlined in Section 3, and the results for the De Pangher long counter are shown in Table 4.1. The mean values for Hunt's earlier efficiency measurements are also given for comparison and the rightmost column (1-HT/JH) contains the ratio, in %, of this work's to Hunt's efficiency values. There is reasonable agreement between the two sets of results, although Hunt's results for ^{252}Cf and ^{241}Am-Be are both just over 2% higher than the present results. The output file of the PCINVFIT analysis of the present ^{252}CF measurement is shown in Appendix A where it can be seen that all the criteria for a good fit and good data (discussed in section 3) are satisfied.

Table 4.1 Efficiency and effective centre results from the De Pangher long counter measurements with sources, and a comparison of the present efficiency results (HT) with those of Hunt (JH).

Source	Gradient	Intercept	Effective Centre (cm)	Efficiency (cm^2) HT	Efficiency (cm^2) JH	1-HT/JH %
^{252}Cf	2.18E-04 ± 8.87E-08	6.90E-04 ± 2.08E-05	3.17 ± 0.10	3.39 ± 0.02	3.47 ± 0.03	2.25
Am-Be	1.25E-03 ± 1.84E-06	5.70E-03 ± 3.29E-04	4.59 ± 0.26	3.21 ± 0.02	3.29 ± 0.03	2.36
Pu-Li	2.00E-03 ± 4.04E-06	7.00E-03 ± 1.00E-03	3.49 ± 0.50	3.45 ± 0.02	3.41 ± 0.03	-1.23
Am-F	5.09E-03 ± 2.29E-05	2.07E-02 ± 5.06E-03	4.07 ± 0.99	3.50 ± 0.04	-	-

The efficiency and effective centre results are plotted in Figures 4.1 and 4.2 respectively. Table 4.2 shows the results obtained from all ^{252}Cf measurements carried out by Hunt in the 1970's and 1980's compared to results from the present work and to values measured by More [13]. All are for the same long counter. It highlights the reproducibility of the earlier measurements of Hunt for the efficiency, and the consistently higher, and slightly more varied, results for the effective centre.

Table 4.2: Efficiency and effective centre results for the De Pangher long counter with a ^{252}Cf source as measured by Tagziria, Hunt and More.

Author	Measurement	Efficiency (cm^2)	Effective Centre (cm)
Hunt	1972-83		
	19-20/12/1972	3.49 ± 0.01	5.66 ± 0.29
	01-11/10/1974	3.49 ± 0.02	6.58 ± 0.50
	09/04/1981	3.48 ± 0.01	4.75 ± 0.33
	12/09/1983	3.41 ± 0.02	6.24 ± 0.38
	11/11/1983	3.45 ± 0.01	5.24 ± 0.42
	05/04/1985	3.46 ± 0.01	5.13 ± 0.21
	1976 (RS5)	3.52 ± 0.02	6.27 ± 0.61
	Average (Hunt)	**3.47 ± 0.03**	**5.70 ± 0.80**
More	BM 1989	**3.32 ± 0.02**	**3.76 ± 0.28**
Tagziria	HT 1997	**3.39 ± 0.02**	**3.17 ± 0.10**
	Average(HT+BM+JH)	**3.40 ± 0.06**	**4.21 ± 1.79**

Although there appear to be discrepancies in the final results for the efficiency and the effective centre, it can be shown that there is little difference between Hunt's measurements (JH) and the present ones (HT) if the efficiency is coupled to the effective centre as measured by the same author. From equation (1) and (4) in section 3, one can write that:

$$\frac{[C_t(r) - C_i(r)]F_a(r)}{QF_I} = \frac{\varepsilon}{4\pi(r + r_o)^2} \qquad (5)$$

For both Hunt's and the present analyses, the left hand sides of equation (5) should be equal and hence:

$$\frac{\varepsilon_{HT}}{(r + r_{oHT})^2} = \frac{\varepsilon_{JH}}{(r + r_{oJH})^2} \qquad (6)$$

where $\varepsilon_{JH}, r_{oJH}$ and $\varepsilon_{HT}, r_{oHT}$ are the efficiency and effective centre as measured by Hunt and Tagziria, respectively.

Table 4.3 shows values of the both sides of equation (6) (column labelled HT and JH) as a function of the distance r for ^{252}Cf measurements. The efficiency and effective centre values are taken from Table 4.2. The fourth column in Table 4.3, equal to 1-JH/HT (in %), shows good agreement between the two measurements for distances above about 1.25 m which is in fact the range over which the measurements were made for these experiments, and over which fluence determinations using the shadow cone technique are normally made.

Table 4.3: Comparison of Hunt's measurements for ^{252}Cf with the present work using equation (6) as discussed above.

Distance (cm)	$\varepsilon\ /(r+r_0)^2$ HT	$\varepsilon\ /(r+r_0)^2$ JH	1-JH/HT %
50	1.1991E-02	1.1185E-02	6.73
75	5.5478E-03	5.3282E-03	3.96
100	3.1849E-03	3.1058E-03	2.48
125	2.0636E-03	2.0313E-03	1.56
150	1.4449E-03	1.4314E-03	0.94
175	1.0679E-03	1.0627E-03	0.49
200	8.2126E-04	8.2009E-04	0.14
250	5.2890E-04	5.3072E-04	-0.34
300	3.6883E-04	3.7131E-04	-0.67
350	2.7179E-04	2.7426E-04	-0.91
400	2.0856E-04	2.1082E-04	-1.09
450	1.6507E-04	1.6710E-04	-1.23
500	1.3390E-04	1.3569E-04	-1.34

In table 4.4 a comparison is given of the present effective centre results for radionuclide sources with measurements made for De Pangher long counters by other workers [14-18]. These include measurements made by Hunt [6,14] with various sources, and a measurement by More [13] using a ^{252}Cf source, all performed at NPL using the same De Pangher long counter as the one investigated in the present work. The remainder of the measurements were for other counters, but, because of the tight manufacturing tolerances applied when constructing this type of long counter, every one should have a very similar effective centre value. The agreement between the various values is not, however, particularly good with disagreements well outside the quoted uncertainties. For ^{252}Cf and ^{241}Am-Be, Hunt's results are significantly higher than the others although his measurements were completely repeatable for ^{252}Cf as demonstrated in Table 4.2. The reasons for the differences between the results of different experimentalists are not clear, although the derived effective centres can be very sensitive to small changes in the data set.

The sensitivity of the effective centre and efficiency of the De Pangher long counter to parameters such as the in-scatter counts and the dead time was investigated. It was for instance found that an overall increase of 3 % in the in-scatter counts resulted in 36% decrease of the effective centre whereas the efficiency decreased by less than 2%. The sensitivity of the effective centre and the efficiency to the dead time of the counting system (a 10 μs fixed dead time in the present case) was found to be less pronounced.

The effective centre is also very dependent on the scatter correction model used in the analysis. It should be noted that some of the earlier measurements listed in Table 4.3 (Thomson, Massand, De Pangher and Mijnheer) were analysed using scatter correction models which had not been fully validated, and have since been shown not to be appropriate in all calibration rooms.

Table 4.4: The effective centre, for several radionuclide sources, as measured by various authors for different De Pangher long counters.

	Code	^{252}Cf	Am-Be	Am-B	Am-F	Pu-Li	Am-Li	Ra-Be	Sb-Be
Tagziria 98	1	3.17±0.10	4.59±0.26		4.07±0.99	3.49±0.50			
Hunt 76	2	5.67±0.80	8.12 ±0.26	6.73±0.78		1.82±0.62	1.52±1.78	2.39±2.16	2.70±1.70
More 89	3	3.76±0.28							
Thomas 91	4	3.80±1.00	9.90±1.00						
Hunt 89	5	4.20±1.00	5.13±1.76						
Taylor 97	6	3.00 ±1.20	4.60±1.60						
Thomson	7		7.74±0.31					2.10±2.04	-0.14±1.02
Massand	8	3.78±0.20	6.17±0.38						
De Pangher	9		5.25±0.20					1.65±0.10	1.65±0.30
Mijnheer	10	3.85±0.30	5.85±0.40				2.45±0.20		1.35±0.20
Heinzelmann	11	4.70 5.80	5.30 6.30				3.70 4.80	3.20 4.00	2.60 4.00

Code:

1: Tagziria 1998, this work.
2: Hunt 1976, references 6 and 14 in this work
3: More 1989; reference 13 in this work
4: Thomas 1991; measurement on customer's counter
5: Hunt 1989; measurement on customer's counter
6: Taylor 1997, measurement on customers' counter
7: Thomson 1972, reference 15 in this work
8: Massand 1972, reference 16 in this work
9: De Pangher 1947, reference 4 in this work
10: Mijnheer 1972, reference 17 in this work
11: Heinzelmann, 1973, reference 18 in this work (values from two theoretical curves)

Considering only the NPL measurements for the present counter, and looking for possible reasons for the discrepancies, it may be noted that modifications to the detector and source support stands at NPL have occurred since Hunt's measurements. Provided, however, that the shadow cone technique correctly subtracts the in-scatter component, these changes should not affect the measurements. Luckily, the results for the efficiency derived from the analysis are not critically sensitive to the values deduced for the effective centre, and a reasonably accurate estimate of the efficiency can still be made. The effective centre problems are further addressed in Section 5.4.

4.2 The NPL Long Counter

Results of efficiency and effective centre measurements and evaluations for the NPL long counter are given in Table 4.5 and in Figures 4.3 and 4.4 respectively, together with those of Hunt [6,14]. The efficiency results of this work agree very well (within 1 %) with those of Hunt for the NPL counter. A summary of all measurements carried out on the NPL long counter, both in this work and by Hunt, is given in the Appendix B.

Table 4.5 Efficiency and effective centre results from the NPL long counter measurements with sources, and a comparison of the present efficiency results (HT) with those of Hunt (JH).

Source	Gradient	Intercept	Effective Centre (cm)	Efficiency (cm^2)		1-HT/JH %
				HT	JH	
^{252}Cf	1.05E-04 ± 6.36E-08	9.45E-05 ± 1.22E-05	0.90 ± 0.12	12.51 ± 0.07	12.65 ± 0.07	1.11
Am-Be	6.44E-04 ± 8.53E-07	2.30E-03 ± 1.79E-04	3.57 ± 0.28	12.12 ± 0.08	12.15 ± 0.10	0.24
Am-B	1.50E-03 ± 2.22E-06	4.00E-03 ± 4.76E-04	2.66 ± 0.32	12.31 ± 0.08	12.35 ± 0.17	0.33
Pu-Li	1.05E-03 ± 5.53E-06	3.80E-03 ± 1.38E-03	2.63 ± 1.31	12.49 ± 0.15	12.22 ± 0.09	-2.18
Am-F	2.69E-03 ± 7.13E-06	1.30E-03 ± 1.80E-03	0.50 ± 0.67	12.49 ± 0.09	-	-

5. MONTE CARLO MODELLING OF THE LONG COUNTERS

5.1 MCNP N-Particle Transport code

5.1.1 Introduction

MCNP[19] is the most widely used general purpose Monte Carlo N-Particle transport code with more than 3000 users world-wide. It was first developed at the Los Alamos National Laboratory in 1943 (the time of the Manhattan project) and has been greatly improved over the years. It now represents an impressive 450 person-years of development. It is used for radiation transport calculations as well as for criticality and reactor physics analyses. MCNP is a continuous energy, generalised geometry, time dependent, coupled or de-coupled, neutron/photon/electron Monte Carlo code. It is obtainable either directly from the Radiation Shielding Information Centre, RSIC, at the ORNL, or via the NEA data bank in Paris, together with a full set of cross section data such as ENDF/B-VI and ENDL [20-24], all on a CD-ROM. The energy regime is from 10^{-11} to 20 MeV for neutrons which can be extended to 100 MeV for some elements using cross section data from the LA100 library, and 1 keV to 1 GeV for photon and electron transport.

An input file created by the user is required from which MCNP reads information about the model such as the geometry, materials, cross sections, radiation source specifications, types of answers or tallies to be obtained, together with any variance reduction (acceleration) techniques the user chooses to apply in order to improve efficiency. With the release of MCNP version 4B in April 1997, twelve new features have become available to users including: the introduction of the enhanced electron physics of ITS3 [25], the production of postscript plot files, a cross section plotting facility with the possibility of dumping to a file an ASCII listing of plotting points, and the new PERT card. The PERT card, which is a major new feature in MCNP-4B, uses a differential operator technique[19,26] to estimate differences due to changes (perturbations) in cross section data, material density and composition. The error on the estimator is always bounded, and both the 1st and 2nd order terms are included. As implemented in the present versions, the PERT card has some limitations; these will be removed in the next version, MCNP-4C, which is presently being developed, and will be released in about two years. The reader is directed to read the MCNP-4B manual for a more complete and comprehensive description of the code, how to use it, its physics, cross section data and features.

5.1.2 MCNP Statistical Analysis

MCNP has arguably the most robust statistical analysis package of all Monte Carlo codes. In addition to the usual mean and variance, the user is provided with the variance of the variance (VOV), which involves the first four history score moments, and represents the error of the error. The tally score probability density function (pdf) is estimated, and ten statistical checks are incorporated to avoid false convergence [19,27]. The latter is characterised by the non existence of the variance or mean (1st and 2nd moments) and thus a failure to satisfy the central limit theorem, which is the most fundamental principle in the Monte Carlo method. By inspecting the slope of the tail of the underlying tally score pdf one can estimate the number of moments that exist, and hence determine whether the VOV, the variance, and even the mean, exist. The VOV is more sensitive to large history scores and should decrease as 1/n, where n is the number of histories.

5.1.3 Accuracy, Precision and Efficiency

Accuracy, precision, and efficiency have very precise meanings when applied to MCNP results. Often called 'systematic error', accuracy is a measure of the difference between the calculated result and the true value of the observable being estimated. It cannot be directly estimated by Monte Carlo codes. The accuracy of the end result depends on the quality of the code, especially its physics, how well the problem is modelled, e.g. in its geometry and source, and it also depends on user errors or abuse of the tools available. Precision, or the 'relative error', which represents the uncertainty in the final result due to statistical fluctuations in the individual samples can, in contrast, be estimated by Monte Carlo codes. The user can control precision by a careful selection of features such as: forward versus adjoint calculations, tally types, variance reduction techniques, and the number of histories run. The speed with which the desired precision is achieved is a measure of the efficiency. A parameter known as the Figure Of Merit (FOM) and defined as:

$$FOM = \frac{1}{R^2 T}$$

where R is the relative error and T is the computing time gives a measure of the efficiency. Since R^2 and T are proportional to 1/n and n (number of histories run) respectively, one would expect the FOM to be constant with n. This constitutes one of the statistical checks to be passed. Other tests for instance are: that the relative error should be less than 0.1 and decreasing, and the pdf slope is more than 3. The larger the FOM, the higher the efficiency. This can be affected by: history scoring efficiency, dispersion in non-zero history scoring, and computer time per history. Although, it is recognised that a safe use of various adequately chosen variance reduction techniques[28] results in increased efficiency, it was judged unnecessary in this problem, and a pure analogue simulation was used. For a comprehensive description and discussion of the problems of various MCNP variance reduction techniques references 19 and 28 are highly recommended. MCNP-4B includes a factor which takes into account the CPU of the computer in use, a so called signal to noise ratio.

5.2 MCNP Models of the Long Counters

5.3 The Geometry

An extensive Monte Carlo modelling of both detectors was carried out using MCNP-4B. The models were constructed from engineering drawings supplied by Centronic (for the De Pangher counter) and by the NPL engineering services for the NPL long counter. In addition, the BF_3

tube of the De Pangher long counter was X-rayed to obtain, or confirm, details of the internal construction. Over 55 'surface' cards and 35 'cell' cards were needed to describe the counters, including their BF_3 tubes, in every detail. The space between the source and the front face of the inner polyethylene moderating block, to which the source to counter distance is usually measured, was modelled as being a void. The stand on which the counters sat was not included in the model as it was considered part of the scattering environment and thus taken into account by the shadow cone correction. The eight holes within the NPL long counter polyethylene, or the corresponding annular trough for the De Pangher counter, were filled with air as they were considered to be an integral part of the counters.

5.3.1 The Source Definition

The source card used for monoenergetic runs was of the form:

```
SDEF ERG=n SUR=m POS = x y z  RAD=D1  DIR=1
SI1    r
```

which represents a mono-directional source of energy n in MeV, emitted from a plane surface, m, in the direction of the positive normal. The surface is positioned a few cm from the front face of the counter, and the point from which each neutron history is started is obtained by uniform sampling over an area on the surface of radius r (taken equal to the counter's radius) thus providing the required starting co-ordinates x, y, z.

For the radioactive sources the ISO[12] recommended spectra were used for ^{241}Am-Be, ^{252}Cf and ^{241}Am-B, whereas a spectrum measured by Tagziria [29] was used for the ^{241}Am-F source. For the ^{238}Pu-Li calculation the ^{241}Am-Li spectrum of Tagziria[29] was used as the best available approximation. It must be noted that using the approximate Watt spontaneous fission spectrum for ^{252}Cf, as suggested in appendix H3 of the MCNP manual, with the parameters a and b equal to 1.025 and 2.926 respectively, gave an efficiency about 2.5% lower than with the ISO or ENDF spectra. The ISO ^{252}Cf spectrum corresponds to a Maxwellian fission spectrum with the energy parameter set to 1.42 MeV, and this can be replicated exactly in MCNP by setting the parameter, a, on the SP card equal to 1.42.

For a radioactive source run the source card was of the form:

```
SDEF SUR=m ERG=D1 RAD=D2 POS=x y z  AXS=1 0 0  DIR=1
SI1    h  energy bins....
SP1    d  probabilities
SI2    r
```

5.3.2 Cross Sections Data

The latest ENDF/B-VI and ENDL cross sections libraries, obtained from the NEA data bank, were used for the various material which make up the counters. In this problem, where thermalisation, including the tracking of neutrons with energy less than 4 eV, is involved, the thermal $S(\alpha,\beta)$ tables were invoked using the MT (poly.01T) card to model the neutron scattering. This allows for the binding of the scattering nucleus in the moderator (polyethylene) since the isotope scattering data is overridden if the neutron energy is in the $S(\alpha,\beta)$ energy range[19]. A plot of the ENDF/B-VI carbon cross section versus energy as used in MCNP is shown in Figure 5.1 which can be compared with that from the BNL325 evaluation used empirically by Hunt in the previous calibrations. The differences and extra details are immediately evident.

5.3.3 The Tallies

MCNP may tally any quantity of the form

$$C\int \varphi(E)f(E)dE$$

where C is an arbitrary normalisation scalar, $\varphi(E)$ is the fluence as a function of energy, and $f(E)$ is either a sum or a product of quantities in the cross section libraries, or it can also be a response function provided by the user. The track length estimate tally (F4:n) with a tally multiplier FM4 (-1   3   107) was used to give the α-particle production, through the $^{10}B(n,\alpha)$ reaction, per cm^3 in the BF_3 active volume per starting particle history. From this the efficiency of the long counter was deduced for the five radioactive sources and for about 200 monoenergetic energies. To obtain the efficiency, directly in the MCNP output file, the first factor, (-1) in the tally multiplier, is multiplied by the product of the effective volume and the area of the surface from which the neutron source spectrum is sampled (equal to πr^2).

5.4 Calculation of the Efficiency of the Long Counters

5.4.1 The De Pangher Long Counter

Over many days, batch files were run continuously on four available PC's to calculate the efficiency of the De Pangher long counter for the radioactive sources which had been measured, and for about 200 monoenergetic energies in the range 1 keV to 20 MeV. No normalisation was applied at this stage through the tally multiplier card. All ten statistical checks of MCNP-4B were passed with 1% relative uncertainty on the tallies, and a Figure of Merit (FOM) of about 130. Each of the above simulations took typically about 90 minutes to process one million histories on an average 166 MHz PC under windows NT. On similar PC's running under Windows 95, it was found this run time could be cut by as much as 40 to 50% if run in a 'DOS only' mode. Table 5.1 shows the efficiency of the De Pangher long counter calculated by MCNP for the radioactive sources compared to measurements made in this work (column labelled HT in Table 5.1) and to the average of all those made at NPL over the years (column labelled All), including the present ones.

Table 5.1: Calculated efficiency of the De Pangher long counter compared to measurements.

Source	Measured		Calculated				
	This work	Mean of All Meas.	Unormalised			Normalised	
	(HT)	(All)	Efficiency (Cal)	1-Cal/HT (%)	1-Cal/All (%)	Efficiency (Nor)	1-Nor/ All (%)
^{252}Cf	3.39 ± 0.02	3.40 ± 0.06	3.28 ± 0.03	3.20	3.29	3.41 ± 0.03	-0.45
Am-Be	3.22 ± 0.02	3.25 ± 0.04	3.15 ± 0.03	1.92	3.09	3.28 ± 0.03	-0.66
Am-F	3.50 ± 0.04	3.50 ± 0.04	3.33 ± 0.03	4.79	4.79	3.46 ± 0.03	1.11
Pu-Li	3.45 ± 0.02	3.43 ± 0.04	3.26 ± 0.03	5.40	4.82	3.39 ± 0.03	1.14

Considering that the counter is more than 30 years old, and that some of the model parameters such as the BF_3 tube pressure, its ^{10}B content, the polyethylene density, etc., can only be known with limited accuracy, the calculations agree well with measurements. It was decided to normalise the MCNP calculations to all efficiency measurements made to date with sources, i.e., including those carried out by Hunt[6,14] and one more recently by More[13]. The ^{238}Pu-Li source was excluded because of the larger uncertainties associated with it. A normalisation of only 3.73% was needed to adjust the calculations to all the source measurements. Figure 5.2 (a) to 5.2 (c) show the MCNP calculated efficiency curves of the De Pangher long counter as a function of energy from 1 keV to 20 MeV, after normalisation, and these can be compared to the original evaluation of Hunt[6]. It can be seen that the efficiency of the long counter is not as flat as is often taken for granted. The prominent structures (dips) in the efficiency curves correspond exactly to resonances in the neutron total cross section of carbon (Figure 5.1) which is the predominant element by weight in the counter. The measured efficiency of the counter for the radioactive sources are also shown in these figures. It should be noted that efficiencies for these sources are plotted at the mean energy, and because of the broad spectra are not necessarily expected to sit exactly on the monoenergetic curves.

Examination of Figures 5.2 (a and b) reveals a broad 'bump' in the MCNP calculated efficiency in the region between 400 and 500 keV. This feature is not present in the efficiency curve for the NPL long counter, see below, and its origins were therefore investigated. The cross section of all materials composing the counters were plotted for inspection, but revealed no obvious explanation for the feature. In terms of materials, the main differences between the two types of long counters is the replacement of the iron casing of the NPL counter by aluminium in the De Pangher counter. The efficiency of the De Pangher counter was therefore re-calculated replacing the aluminium case by an iron one. The results are shown in Figure 5.2 (d) which demonstrates that the structure observed at about 450 keV in the De Pangher long counter efficiency curve is not due to the different casing materials. Since the materials composing both counter are predominantly the same, except for the cases, it must be concluded that this feature is due to dimensional differences in the counters.

5.4.2 The NPL Long Counter

Similar calculations to the above were made for the NPL long counter, each run taking about 120 minutes to process 1 million histories on a 166 MHz PC (Windows NT) with a relative uncertainty of 1% and an FOM of 113. Table 5.2 shows results of the MCNP calculations for the NPL long counter, compared to measurements made in this work (column labelled HT) and to the average of all those made at NPL (column labelled All), including the present. A normalisation of 11.19% was needed to adjust the calculations to all source measurements.

Table 5.2: Calculated efficiency of the NPL long counter compared to measurements.

Source	Measured		Calculated				
	This work	Mean of All Meas.	Unormalised			Normalised	
	(HT)	(All)	Efficiency (Cal)	1-Cal/HT (%)	1-Cal/All (%)	Efficiency (Nor)	1-Nor/ All (%)
^{252}Cf	12.51 ± 0.07	12.58 ± 0.10	10.96 ± 0.10	12.41	12.90	12.34 ± 0.10	1.96
Am-Be	12.12 ± 0.08	12.15 ± 0.02	10.80 ± 0.10	10.90	11.01	12.16 ± 0.10	-0.17
Am-F	12.49 ± 0.09	12.49 ± 0.09	11.14 ± 0.10	10.83	10.83	12.54 ± 0.10	-0.37
Am-B	12.31 ± 0.08	12.33 ± 0.03	11.11 ± 0.10	9.70	9.91	12.51 ± 0.10	-1.41
Pu-Li	12.49 ± 0.15	12.35 ± 0.19	10.51 ± 0.09	15.82	14.91	11.83 ± 0.10	4.22

Figure 5.3 (a) to 5.3 (c) show the MCNP calculated efficiency curves of the NPL long counter as a function of energy from 1 keV to 20 MeV, after normalisation to all source measurements. The measured efficiencies of the counter for radioactive sources are also shown in these figures together with the original evaluation of Hunt.

5.5 Calculation of the Effective Centre of the Long Counters using MCNP

5.5.1 Introduction

When using a long counter to measure the fluence from a point source of neutrons it is crucial that the effective centre is known as accurately as possible. As was noted in the introduction, the determination of this value has always represented a serious challenge to calibration laboratories and users alike. Results often conflicted, were widely spread, and depended on many parameters such as: the person making the measurements, scatter correction methodology, the room size, etc. Bearing in mind these difficulties, there was a need to find an alternative and better way of determining the effective centre of these counters. Having now established a good MCNP model for the long counters it was used to mock up a real experiment as depicted in Figure 2.2 but without the shadow cone. The point source was fixed in position on the axis of the detector and the counter positioned at varying distances from the source. Both source and counter were assumed to be in vacuum and thus the complications of scatter corrections were avoided. The data analysis is then similar to that carried out for the measurements as described in Section 3 except that the scatter counts, system dead time, and air attenuation are zeroed in the input parameters to the PCINVFIT least square fit programme which yields the effective centre.

5.5.2 Validation of the Method

In order to test this new method of determining the effective centre using MCNP, and also to test both the least squares method of analysis described in Section 3, and PCINVFIT, a similar set-up to the above was simulated replacing the long counter with a polyethylene sphere of radius 22 cm (the same radius as the long counter front face). This sphere enclosed at its centre a smaller sphere of radius 4 cm, a void cell (vacuum), for which the fluence tally was calculated, using the track length estimator card F4, for varying point-source-to-centre-of-sphere distances. In a series of computer runs which extended over several days, the F4 tally was calculated for 42 distances ranging from 50 to 600 cm. The inverse of the square root of the tallies are plotted in Figure 5.4 against the source to counter distance. The least squares procedure of Section 3 was applied which resulted in an effective centre which was at a distance of (0.41 ± 0.19) cm from the physical centre of the sphere. Because the source-to-sphere-centre distances extended down to 50 cm, geometry corrections had to be applied to the data. The value used for the 'neutron effectiveness parameter', δ, was that recommended by ISO[10], i.e., 0.5. There is, however, evidence[30] that δ decreases as the sphere size increases. For a δ value of 0.25 the effective centre was within less than 1 mm of the physical centre. In view of the uncertainties in δ, the fact that the effective centre is so close to zero, as would be expected for a spherical system, can be taken as validation of the method of analysis, PCINVFIT, and the new method of determining the effective centre using Monte Carlo simulation.

5.5.3 The Effective Centre of the De Pangher Long Counter using MCNP.

For the long counters, the quantity tallied, namely tally F14, is the same as in Section 5.2.4 except that, because the source is a point source, the tally multiplier includes only the effective

5.5.3 The Effective Centre of the De Pangher Long Counter using MCNP.

For the long counters, the quantity tallied, namely tally F14, is the same as in Section 5.2.4 except that, because the source is a point source, the tally multiplier includes only the effective volume of the BF_3 active region, hence giving the alpha production in this volume per starting particle history, not the efficiency. The inverse square root of the tally, F14, is plotted in Figures 5.5 to 5.7 as a function of source to counter distance, respectively for the ^{252}Cf and the ^{241}Am-Be sources and for 565 keV monoenergetic neutrons. PCINVFIT was subsequently run to yield, as described above, the calculated effective centre. The results are shown in Table 5.3 and Figures 5.5 to 5.7. The simulated effective centres agree well with the present measurements.

Table 5.3 Effective centre of the De Pangher long counter calculated using MCNP for ^{252}Cf, ^{241}Am-Be and for a 565 keV monoenergetic field.

Source	Measured (cm)	Calculated (cm)
565 keV	1.88 ± 0.24	2.20 ± 1.21
^{252}Cf	3.17 ± 0.10	2.75 ± 0.56
^{241}Am-Be	4.59 ± 0.26	4.65 ± 0.94

5.5.4 The Effective Centre of the NPL Long Counter using MCNP

Similar work to that described in the previous Section was carried out for the NPL long counter for ^{252}Cf and ^{241}Am-Be neutron sources and 144 keV monoenergetic field. The inverse of the square root of the tally is plotted in Figure 5.8 to 5.10 against the source-to-counter distance, respectively for the ^{252}Cf and the ^{241}Am-Be sources and for 144 keV neutrons. PCINVFIT was run to yield the calculated effective centre distances shown in Table 5.4 and Figures 5.8 to 5.10. Again the simulated effective centres agree well with the present measurements, except for the case of ^{252}Cf. Although the analysis of the ^{252}Cf measurements has been checked in detail, no obvious error can be found, and the measured result must remain suspect. A new and independent measurement is planned.

Table 5.4 Effective centre of the NPL long counter calculated using MCNP for ^{252}Cf, ^{241}Am-Be and for a 144 keV monoenergetic field.

Source	Measured (cm)	Calculated (cm)
144 keV	−1.76 ± 0.23	−1.28 ± 1.02
^{252}Cf	0.90 ± 0.12	2.58 ± 1.07
^{241}Am-Be	3.57 ± 0.28	3.16 ± 0.74

5.6 Rationale for the Approach used to Calculate the Efficiency

The neutron source term used for the main calculations of the efficiencies was described in Section 5.2.2. It is a surface source, and produces a parallel beam of neutrons incident on the

In normal usage the long counters are employed to determine the neutron fluence from a point source of neutrons at some finite source-to-detector distance. This distance is generally between 1 and 5 m at NPL. The question then arises as to whether the parallel beam approach calculates the efficiency required. The analysis of the sets of calculated data used to estimate the effective centre, as described above, also provides a value for the efficiency, and this can be compared to the value obtained from the parallel beam approach. This has been done for both long counters with the ^{252}Cf and ^{241}Am-Be sources and one monoenergetic neutron field, and the results are shown in Tables 5.5 and 5.6.

Table 5.5: The De Pangher long counter efficiency calculated for parallel and point source radiation fields, prior to normalisation, for ^{252}Cf, ^{241}Am-Be and 565 keV.

Source	Parallel Beam	Point Source	
	Efficiency	Gradient	Efficiency
^{252}Cf	3.28 ± 0.03	1.964 ± 0.005	3.26 ± 0.02
^{241}Am-Be	3.15 ± 0.03	1.996 ± 0.010	3.15 ± 0.03
565keV	3.27 ± 0.03	1.955 ± 0.010	3.29 ± 0.03

There is obviously very good agreement between the two sets of results giving confidence in the parallel beam approach as a way of determining an efficiency value which is valid for a point source, provided the correct effective centre is available. It should be noted, however, that in the parallel beam approach the calculations took of the order of 90 minutes of computing time to determine an efficiency value, whereas the approach involving a multitude of point source calculations took days of computing time.

Table 5.6: The NPL long counter efficiency calculated for parallel and point source radiation fields, prior to normalisation, for ^{252}Cf, ^{241}Am-Be and 144 keV.

Source	Parallel Beam	Point Source	
	Efficiency	Gradient	Efficiency
^{252}Cf	10.96 ± 0.11	1.066 ± 0.005	11.07 ± 0.11
^{241}Am-Be	10.80 ± 0.11	1.075 ± 0.004	10.87 ± 0.09
144 keV	10.05 ± 0.10	1.116 ± 0.015	10.09 ± 0.09

One other 'validation' calculation was performed, whereby, the F14 tally of Section 5.3.2, for an unbiased ^{252}Cf point source sitting at a single position of 200 cm from the De Pangher long counter was calculated for 150 million particle histories. The tally was divided by $4\pi d^2$, where d is the source to counter distance, to yield the efficiency of the counter. It was found that this efficiency coincides with the parallel beam efficiency only if the distance d is increased by 1.77 cm which can be interpreted as an estimate of the effective centre. This is compared to 2.75 cm obtained with the least square method outlined in the above sections which corresponds to an efficiency of (3.31 ± 0.03) cm^2 compared to (3.28 ± 0.03) cm^2 calculated with the parallel beam (see Table 5.5). Although both calculations agree within the uncertainties, both in sign and magnitude, the least squares method, which takes into account calculations for a point source at more than 30 positions, provides a more robust and more physically justifiable method to calculate the effective centre of the long counter.

6. SUMMARY AND FUTURE PROGRAMME

The Monte Carlo technique has become a very powerful tool in radiation transport as users have taken full advantage of richer cross section data, more powerful computers and Monte Carlo techniques for radiation transport, with high quality physics and better known source spectra.

At the National Physical Laboratory the most extensive modelling ever performed for long counters has been undertaken. New and more accurate efficiency curves have been produced for both long counters in use at NPL. The end result will be improved standardisation and calibration accuracies which will benefits customers and users. A novel approach using Monte Carlo radiation transport techniques was developed and validated to determine more accurately the effective centre, as well as the efficiency of the counters.

At the time of writing this report work to extend the effective centre calculations for both long counters in a systematic and extensive way for all radioactive neutron sources measured and for many more monoenergetic neutron sources is gathering momentum. These results will be reported in due course. It must be noted that, within the current programme, it has not been possible to make measurements, as would have been ideal, using low energy radionuclide neutron sources. This makes the MCNP model even more useful, especially at energies where measurements cannot be carried out. These measurements are however planned for the next programme where use of sources such as ^{226}Ra-Be(n,γ) and ^{124}Sb-Be(n,γ) is under consideration.

Acknowledgements: We would like to thank Andrew Bennet and John Winnington for running the Van de Graaff accelerator, often from early morning to late in the day, and Nicky Horwood for typing in many of the data. We are also grateful to Centronic (UK) for providing engineering details of the De Pangher long counter and of the BF_3 tubes. This work was funded by the UK National Measurement System Policy Unit and was Deliverable (v) of Project 2.1 in its 1995 to 1998 Programme for Ionising Radiation Monitoring Metrology.

References

1) Hanson, A.O. and McKibben, J.L. A Neutron Detector Having Uniform Sensitivity from 10 keV to 3 MeV, *Phys. Rev.* 1947, **72,** 673.
2) Knoll, Glenn F, *Radiation Detection and Measurement,* (John Wiley & Sons) Second Edition 1989.
3) McTaggart, M.H, A Study of the Neutron Long Counter, *AWRE report NR/A-1/59,* 1959.
4) De Pangher, J. and Nichols, L.L A Precision Long Counter for Measuring Fast Neutron Flux Density, *Pacific Northwest Laboratory Report BNWL-260,* 1966.
5) Marshall, T.O. Some Tests on the Consistency of the Performance of Six Precision Long Counters Intended as Secondary Standards for the Measurement of Neutron Flux Densities, *Health Physics* , 1970, **18,** 427.
6) Hunt, J.B. The calibration and use of long counters for the accurate measurement of neutron flux density, *NPL Report RS 5,* 1976.
7) Allen, W.D in *Fast Neutron Physics,* ed. Marion and Fowler, Interscience Publishers, Inc, 1960, Vol. 1 page 361.
8) Hunt, J.B. Harrison, K.G. and Wilson, R. Calibration of a De Pangher long counter and two neutron survey monitors at 21.5 keV, *Nuclear Instruments and Methods* 1980, **169,** 477.
9) Hunt, J.B. and Robertson, J.C. The long counter as a secondary standard for neutron flux density, In Proceedings of the *1st Symposium on Neutron Dosimetry in Biology and Medicine, Munich,* 1972, Vol. II p 935.
10) International Organization for Standardization, Draft International Standard, Reference Neutron Radiations: Calibration fundamentals related to the basic quantities characterising the radiation field, *ISO 8529-2.DIS,* 24 February 1998.
11) International Organization for Standardization, International Standard, Neutron Reference Radiations for Calibrating Neutron Measurement Devices used for Radiation Protection Purposes, *ISO 8529* , 1st ed. October 1989.
12) Bardell, A.G. Burke, M. Tagziria, H. and Thomas, D.J Anisotropy of Emission from Radionuclide Neutron Sources, *NPL CIRM Report,* to be published, 1998.
13) More, B. R. calibration records at NPL.
14) Hunt, J.B. private communication, and calibration records at NPL.
15) Thomson, I.M.G. and Lavender, A. Calibration of the De Pangher long counter, *in Neutron Monitoring for Radiation Protection Purposes, Proceedings of a Symposium,* Vienna, 11-15 December1972, Vol. II p 483, Published by the IAEA, 1973.
16) Massand, O.P. Investigation of some Properties of the Precision Long Counter, *Report EUR 4783e, JNRC (now IRMM), JRC-EC* , Geel 1972
17) Mijnheer, B.J. Standard Fluxes and Standard Moderating Counters for Neutron Fluence Measurements, 1972, *IKO Amsterdam, Thesis.*
18) Heinzelmann, M. and Rohloff, F. Das Effektive Zentrum des Long-Counters, *Nucl. Instrum. & Meths* 1973, **109,** 205.
19) Judith F Briesmeister, editor, MCNP - A General Monte Carlo N-Particle Transport Code, Version 4B, edited by RSIC, Oak Ridge National Laboratory. *LANL Manual LA-12625-M Version 4B* (1997) Los Alamos:
Forums: mcnp-forum@lanl.gov (US) or mcnp-l@psi.ch (Swiss),
Web site: http://www-xdiv.lanl.gov/XCI/PROJECTS/MCNP/index.html
e-mail: mcnp@lanl.gov or jfb@lanl.gov
20) Young, P.G. et al. Transport data libraries for incident proton and neutron energies to 100 MeV, *LANL Report LA-11753-MS* (1990) Los Alamos, available on the World Wide Web.
21) Hendricks, J.S. Frankle, S.C. and Court, J.D. ENDF/B-VI data for MCNP, *LANL Report LA-12891* (1994) Los Alamos, available on the World Wide Web.

22) Court, J.D. Brockhoff, R.C. and Hendricks, J.S. Lawrence Livermore Pulsed Sphere Benchmark Analysis of MCNP ENDF/B-VI, *LANL Report LA-12885* (12/1994).

23) Court, J.D. and Hendricks, J.S. Benchmark Analysis of MCNP ENDF/B-VI Iron, *LANL Report LA-12884* (12/1994).

24) Court, J.D., Hendricks, J.S. and Frankle, S.C. MCNP ENDF/B-VI Validation: Infinite Media Comparison of ENDF/B-VI and ENDF/B-V , *LANL Report LA-12887* (12/1994)

25) Halbleib, J.A. Kensek, R.P. Mehlhorn, T.A. Valdez, G.D. Seltzger, S.M. and Berger, M.J. ITS Version 3.0: The Integrated Tiger Series of Coupled Electron/Photon Monte Carlo transport Codes, *SAND91-1634* (3/1992).

26) McKinney G.W. and Iverson J.L., Verification of the Monte Carlo Differential Operator Technique for MCNP, *LANL Report LA-13098* (2/1996).

27) Pederson, S.P., Forster R.A. and Booth T.E., Confidence Interval Procedures for Monte Carlo Transport Simulations, *Nuclear Science and Engineering,* 1997, **127**, 54-77.

28) Booth T.E., A Sample Problem of Variance Reduction in MCNP, *LANL Report LA-10365* (10/1985).

29) Tagziria, H. A Users' Guide for the NPL ^{3}He Neutron Spectrometry System, *Final report for Contract EMRA NPL82/0487* 1993.

30) Hunt, J.B. The Calibration of Neutron Sensitive Spherical Devices, *Radiation Protection Dosimetry,* 1984, **8,** 239-251.

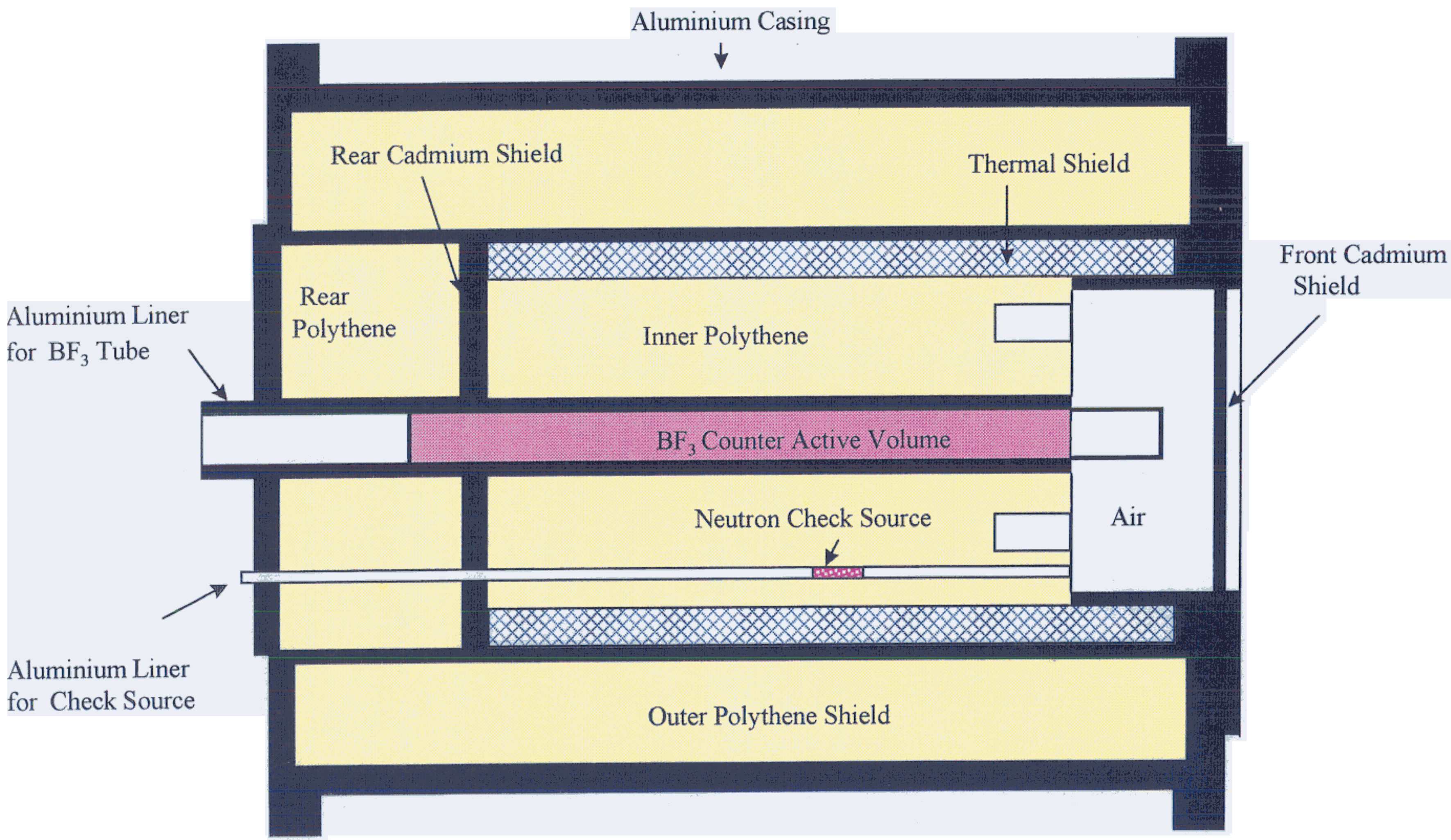

Figure 1.1: Schematic diagram of the De Pangher long counter

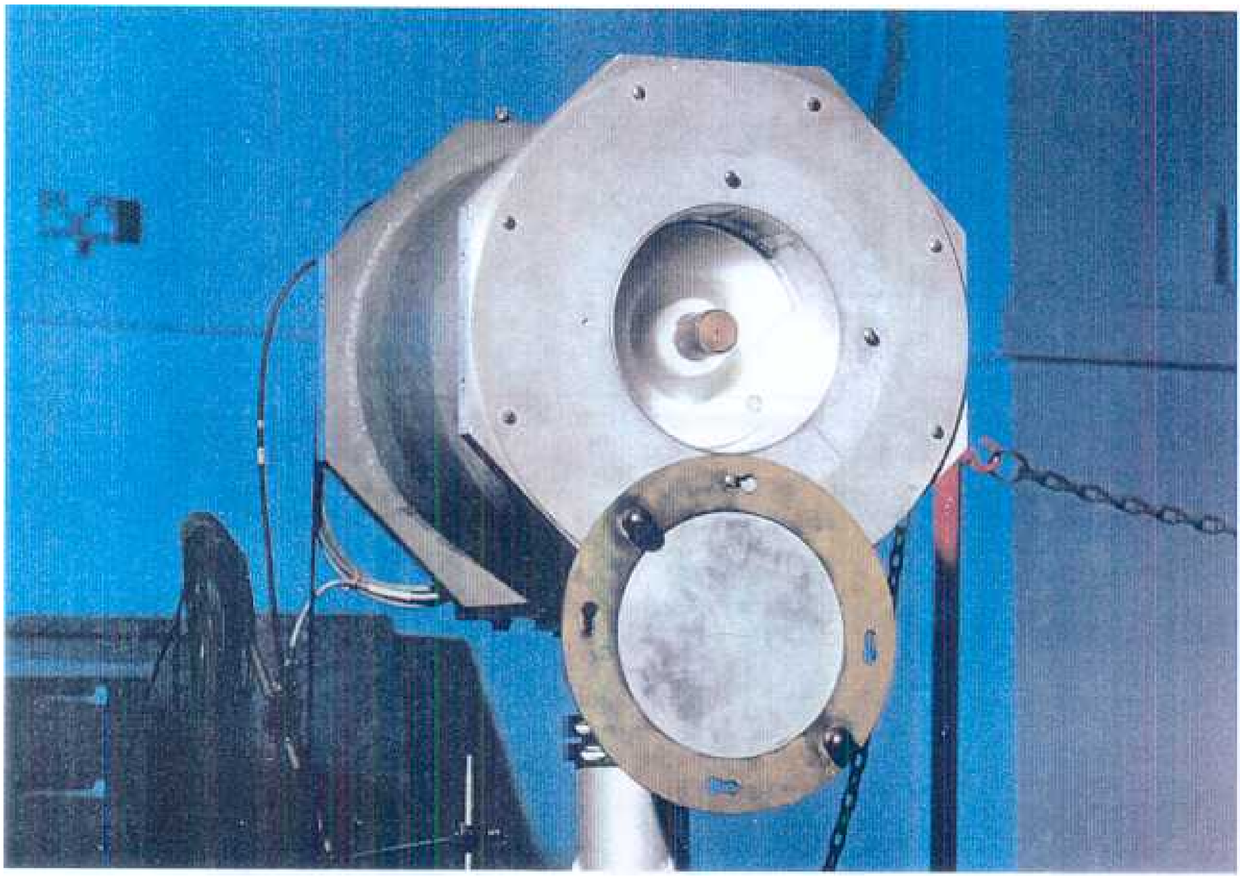

Figure 1.2: The De Pangher long counter with the Cadmium cover dropped

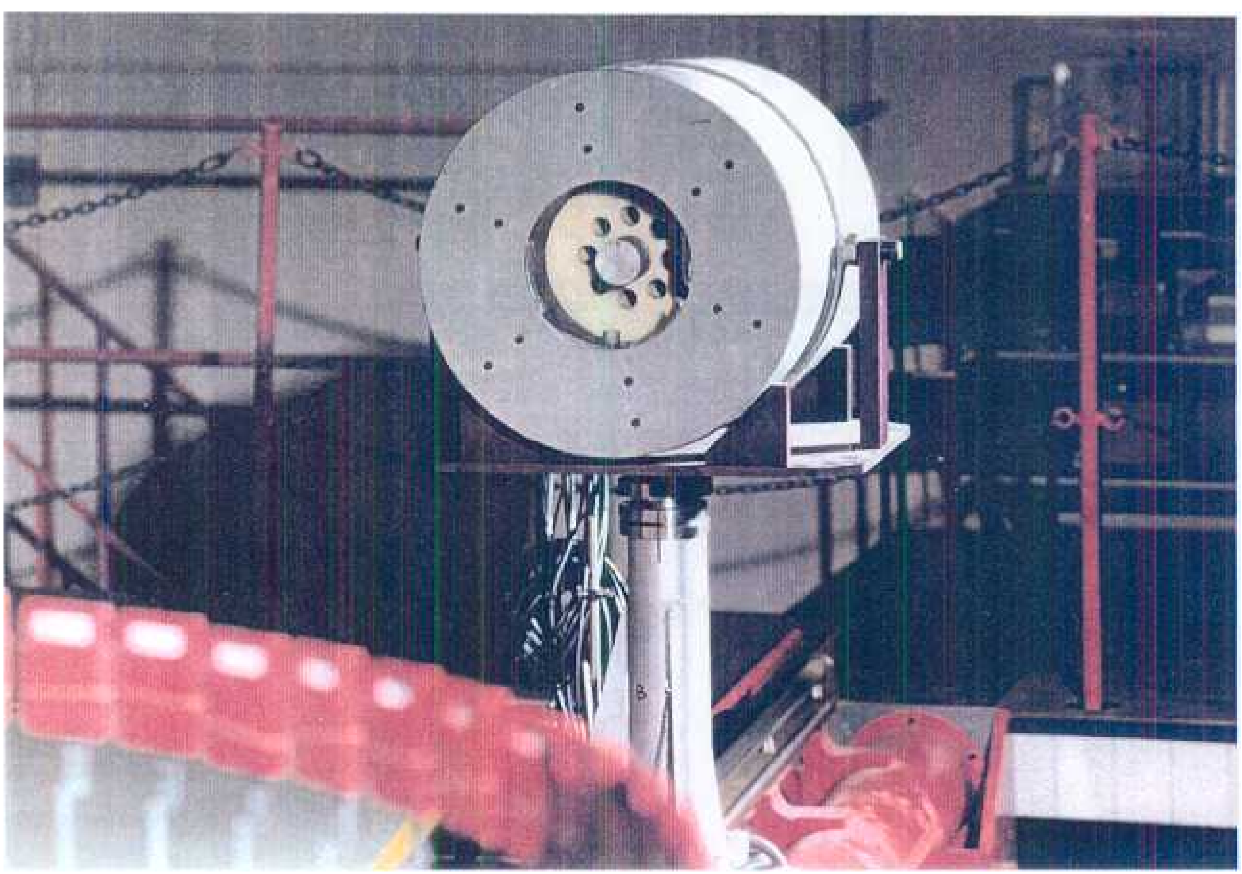

Figure 1.3: The NPL (McTaggart type) long counter

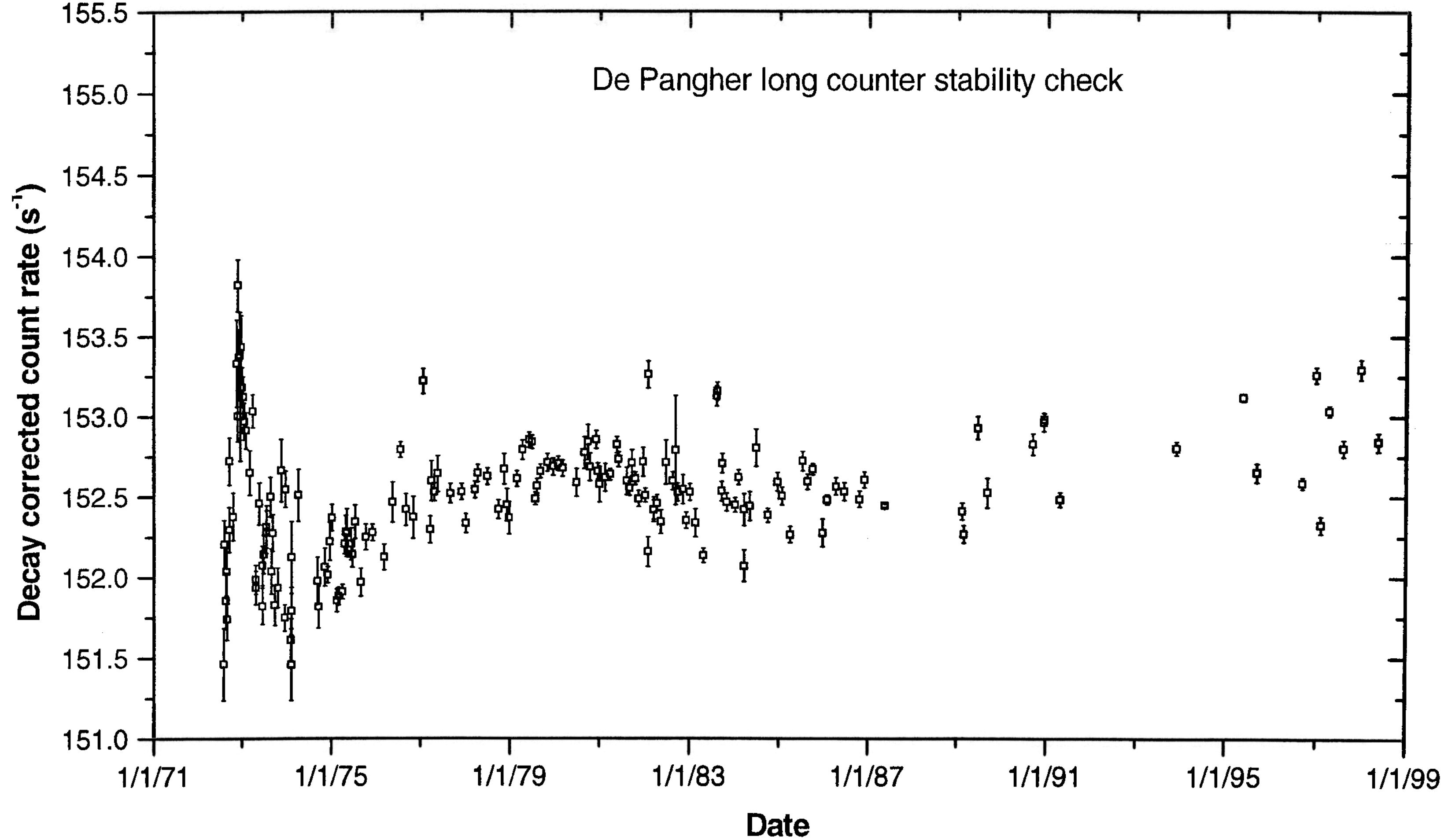

Figure 1.4: De Pangher long counter long-term stability checks showing the variation with time for the decay-corrected count rate from an ^{241}Am-Be source located in a fixed position within the moderator

Cone #	A (cm)	B(cm)	θ°
1	3.2	12.0	5.0
7	9.0	17.0	4.6
8	3.5	20.6	9.7

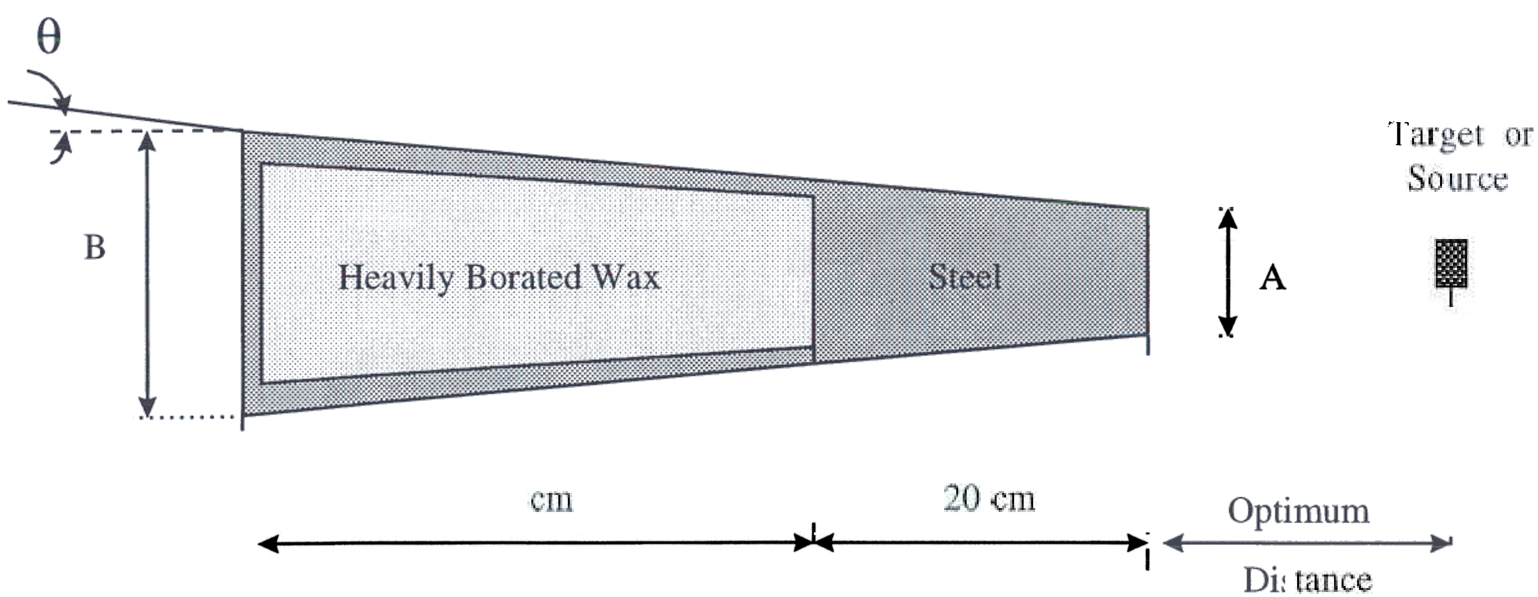

Figure 2 hemati diagram of NPL hadow cones with table showin; d tails of th cones used in this work

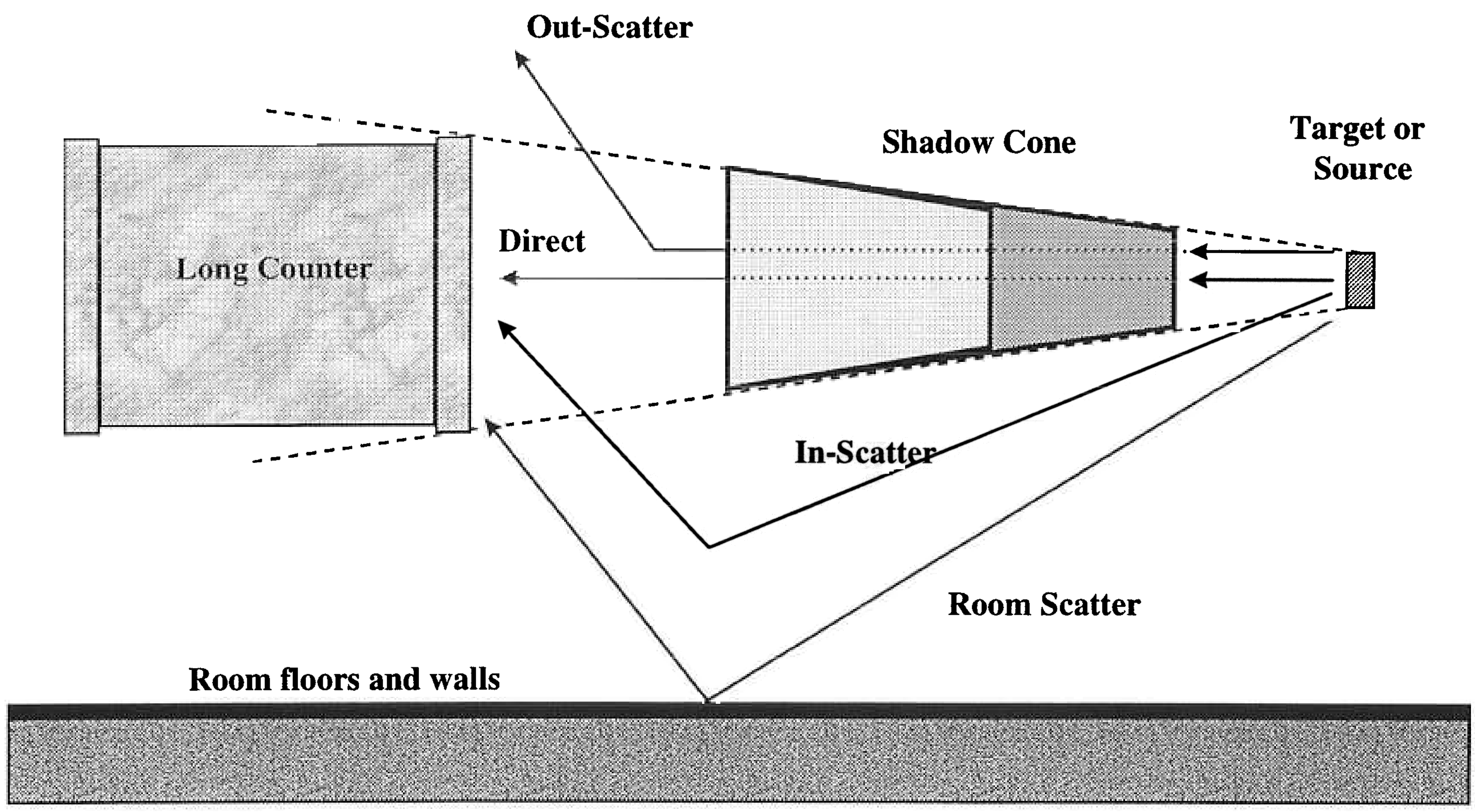

Figure 2.2: Experimental arrangement and scatter components

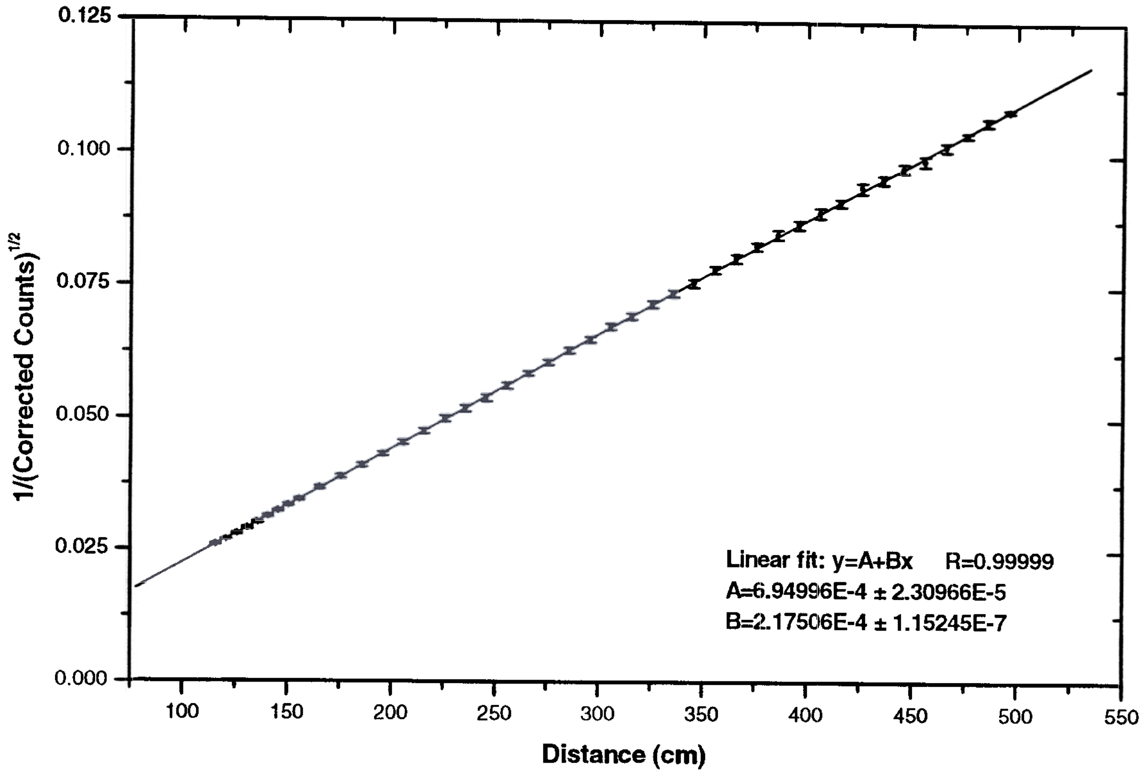

Figure 2.3: Calibration of the De Pangher long counter for ^{252}Cf

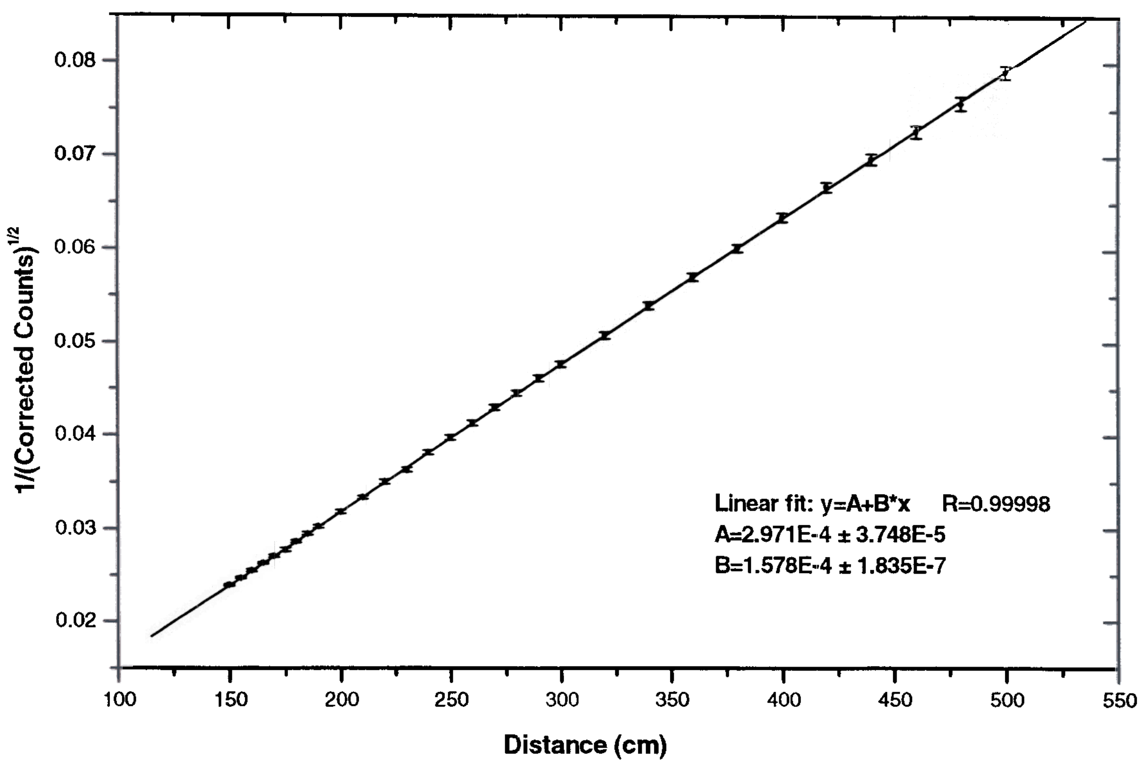

Figure 2.4: Calibration of the De Pangher long counter for 565 keV

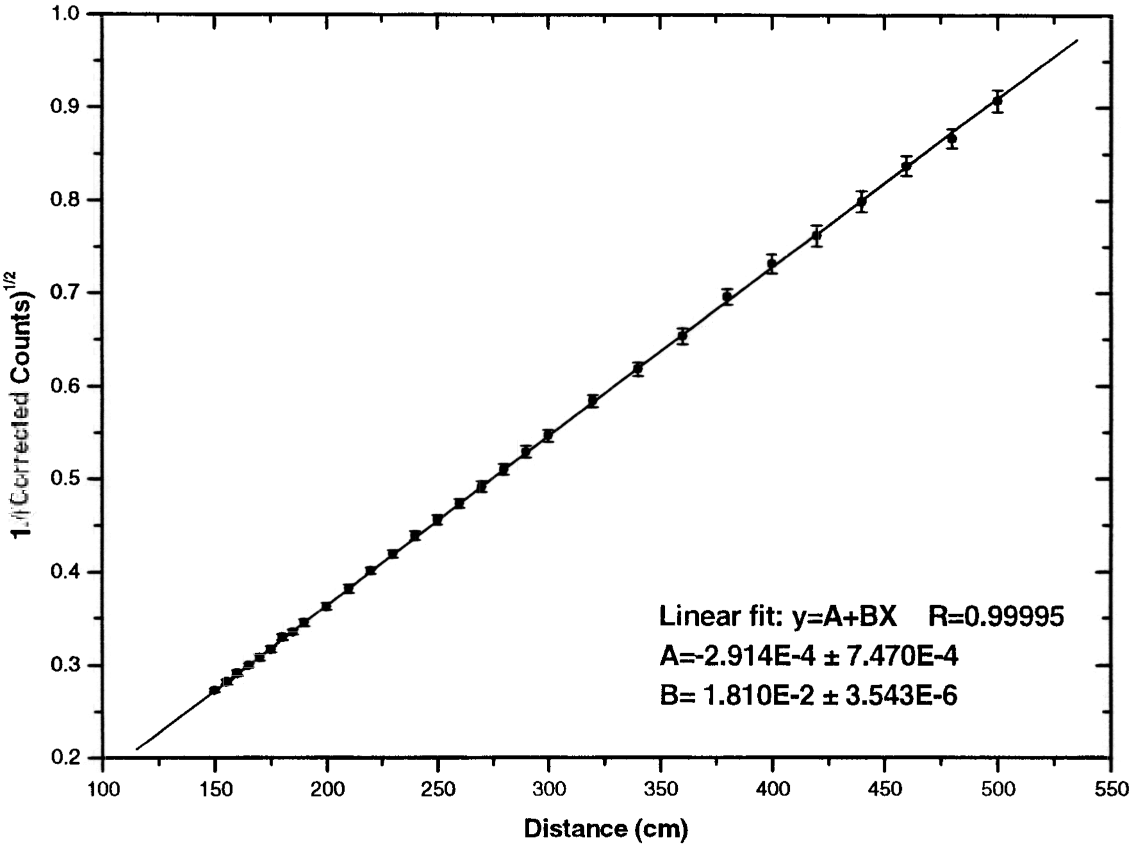

Figure 2.5: Calibration of the De Pangher long counter for 1200 keV

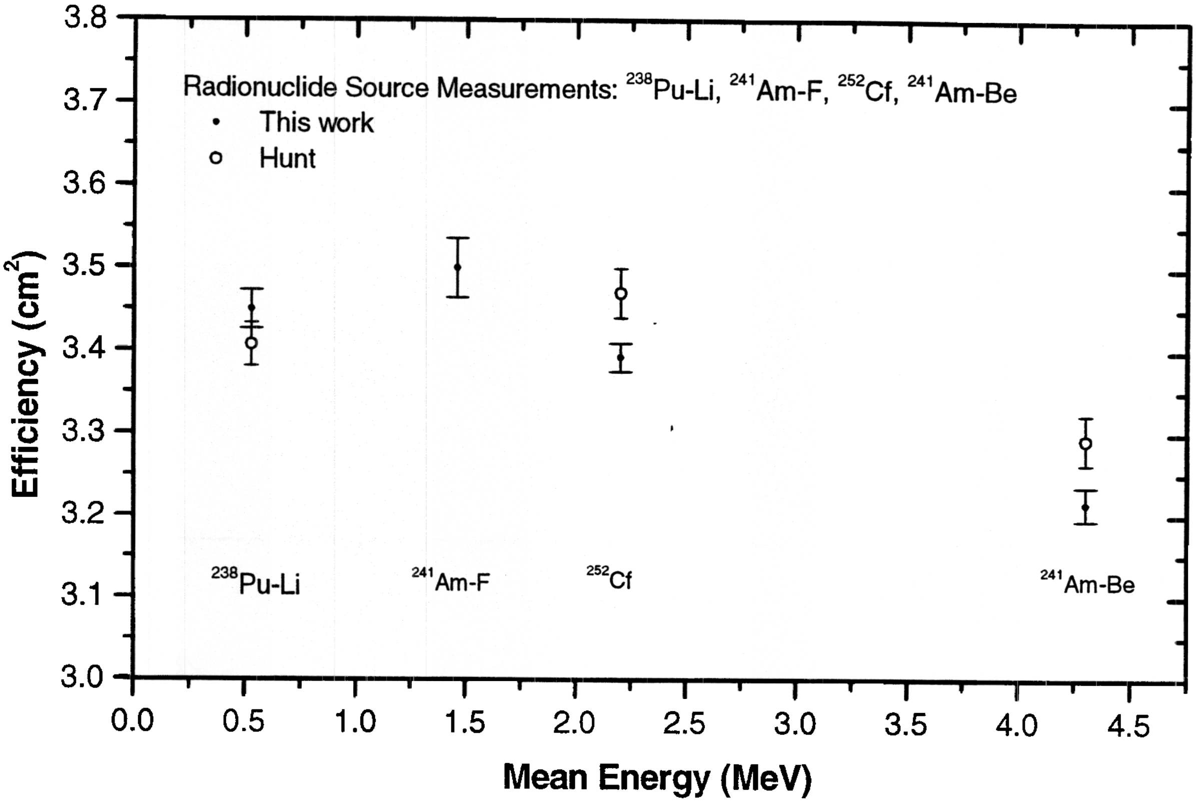

Figure 4.1: Measured efficiency of the De Pangher long counter

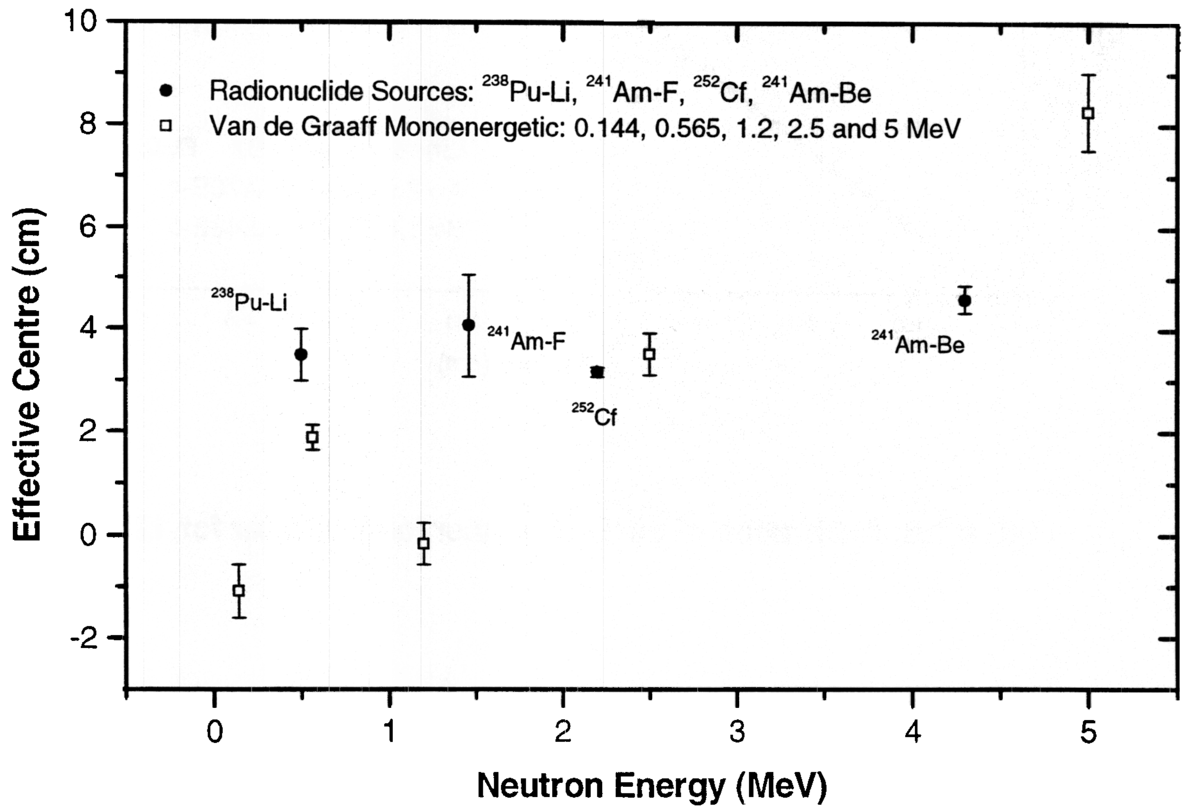

Figure 4.2: Measured effective centre of the De Pangher long counter

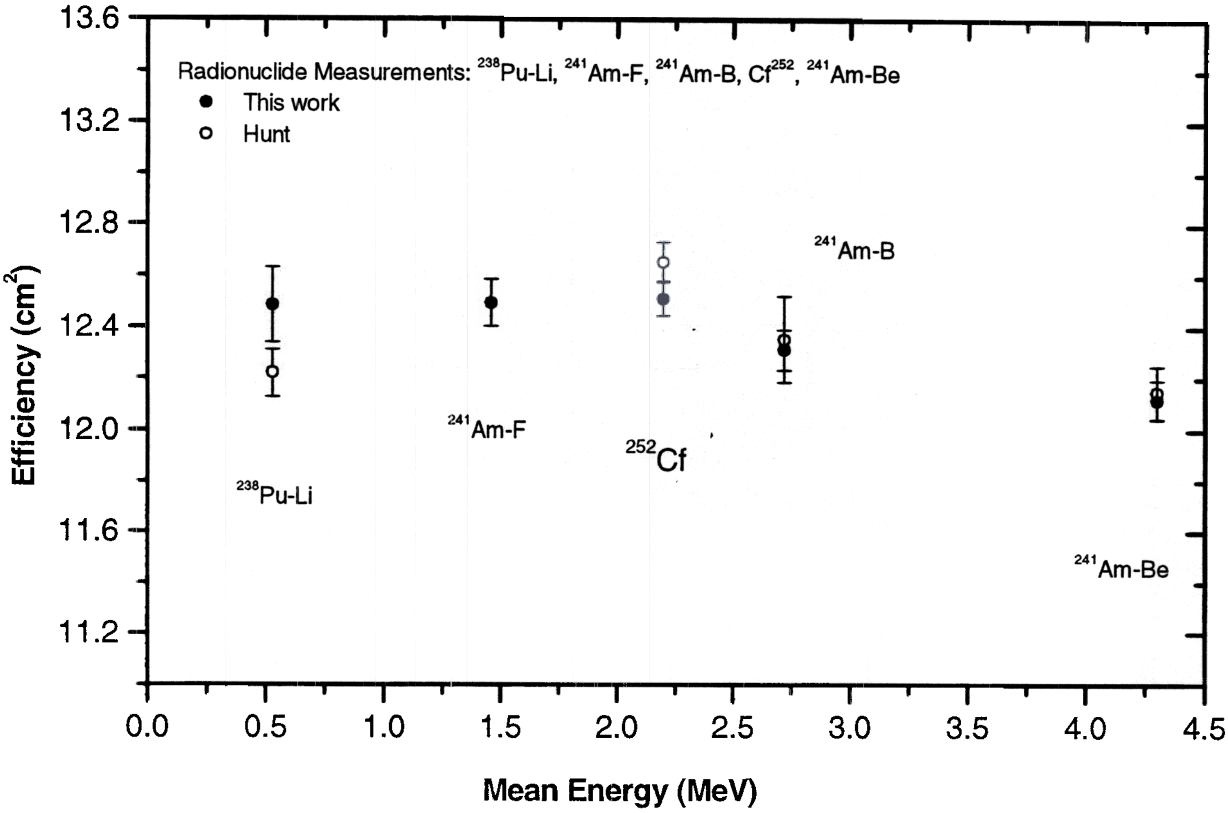

Figure 4.3: Measured efficiency of the NPL long counter

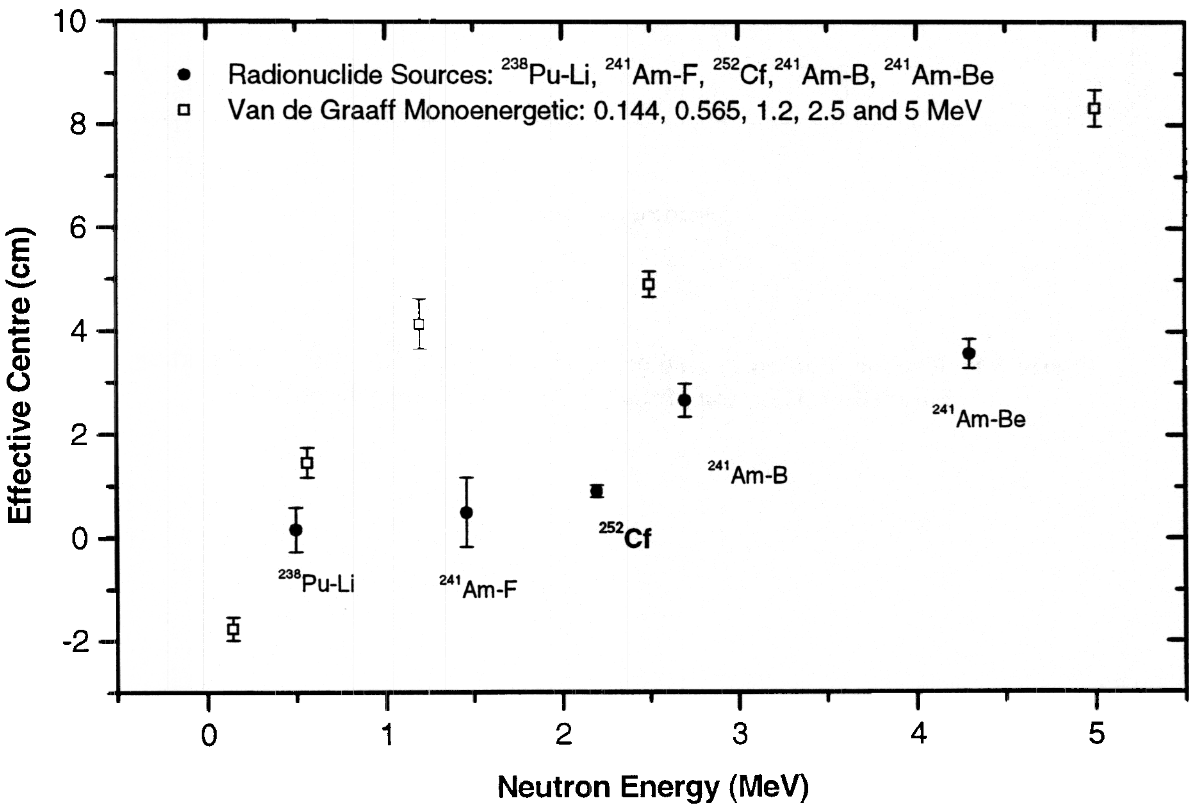

Figure 4.4: Measured effective centre of the NPL long counter

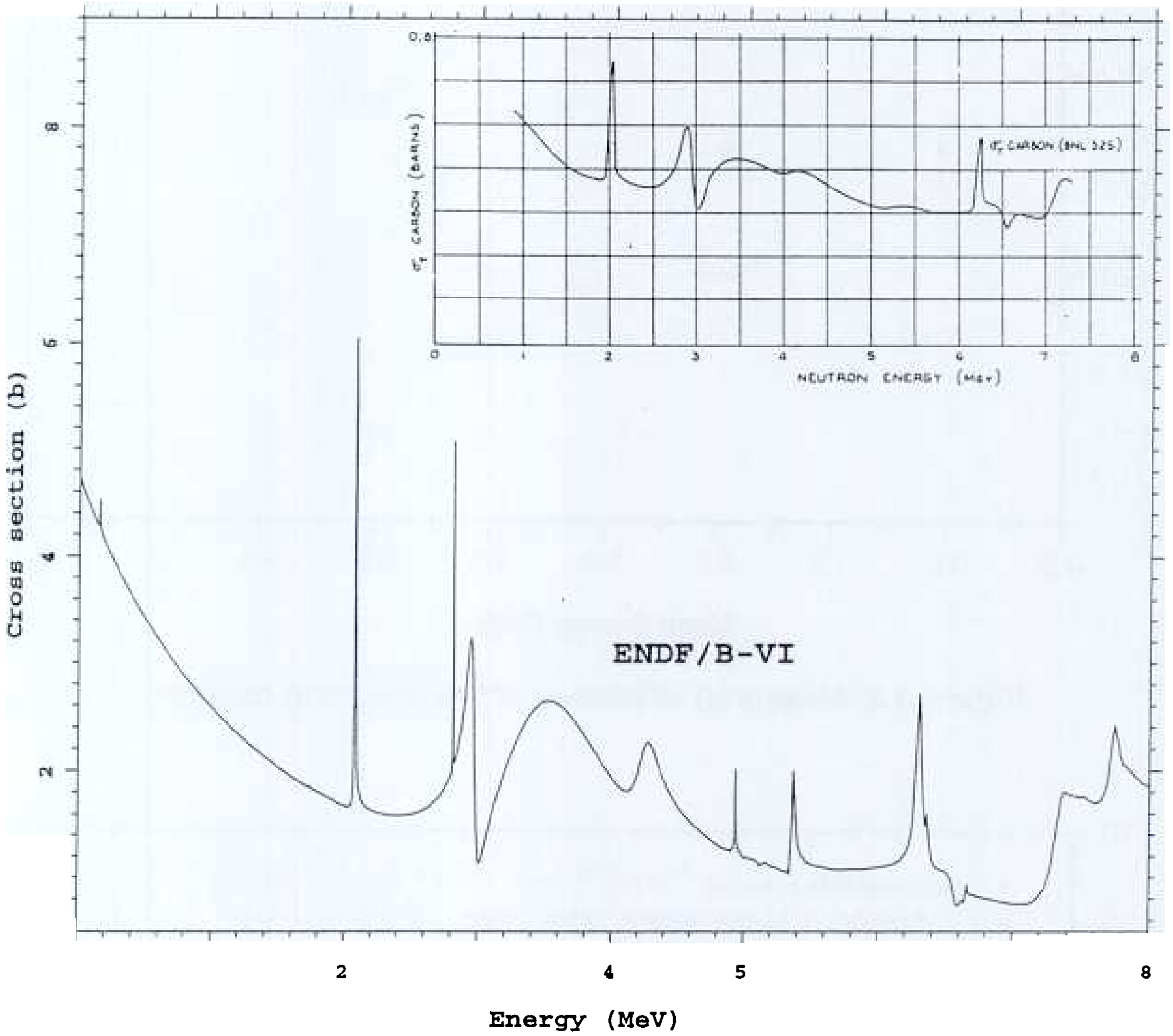

Figure 5.1: Carbon total cross sections used in this work (ENDF/B-VI) and by Hunt (BNL325), top of the figure, taken from reference 7.

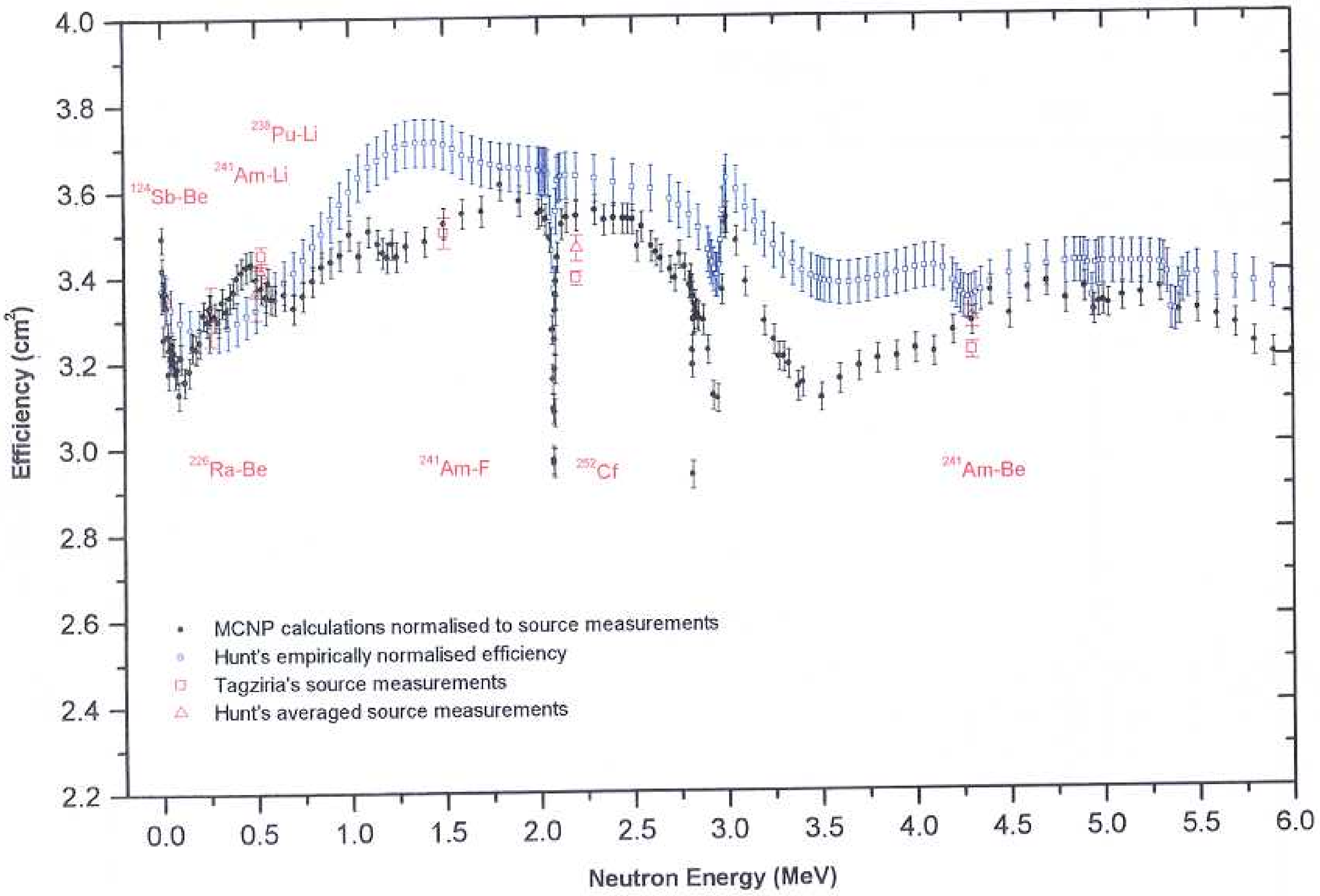

Figure 5.2 (a): Efficiency of the De Pangher Long Counter [0-6 MeV]

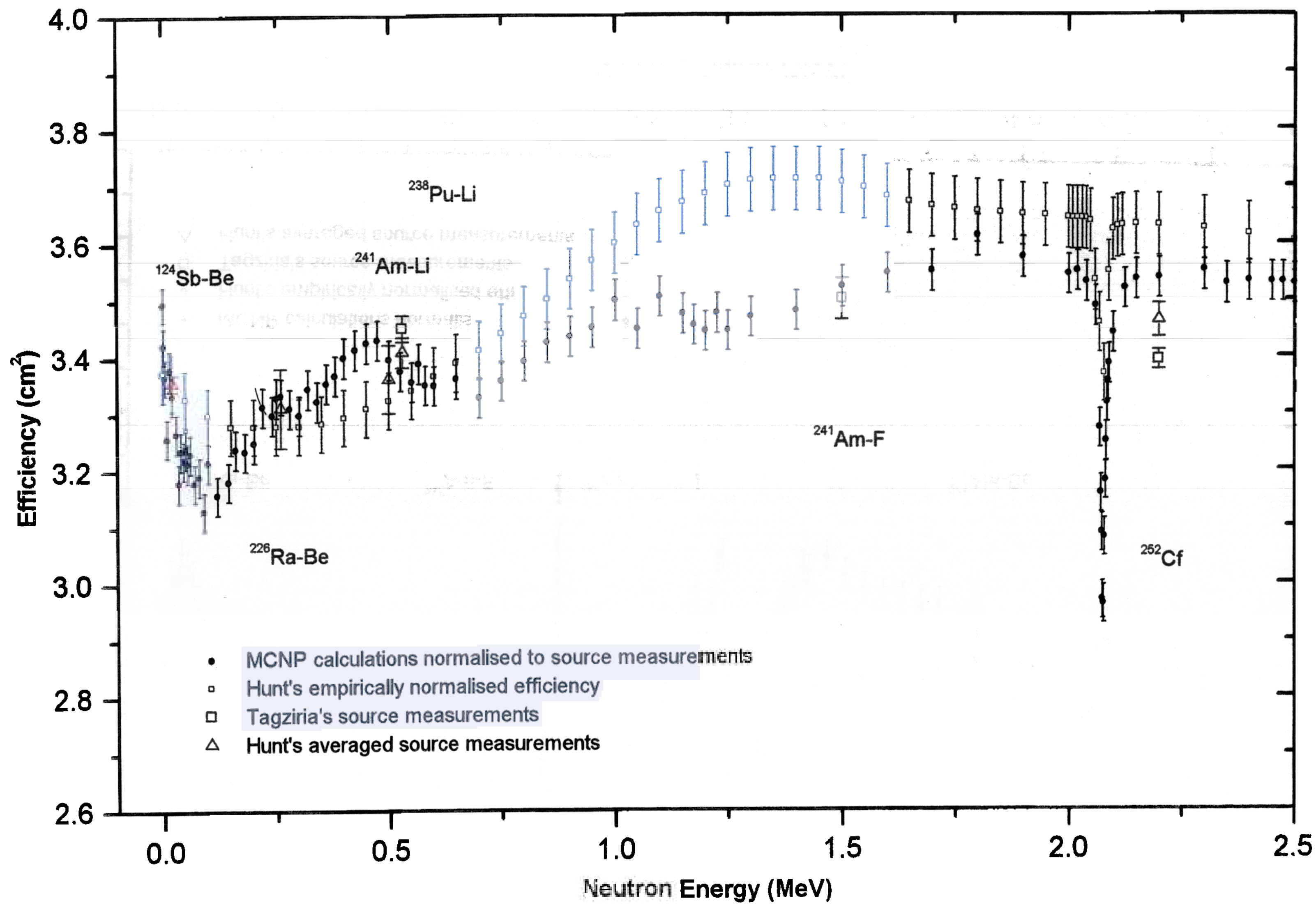

Figure 5.2 (b): Efficiency of the De Pangher Long Counter [0-2.5 MeV]

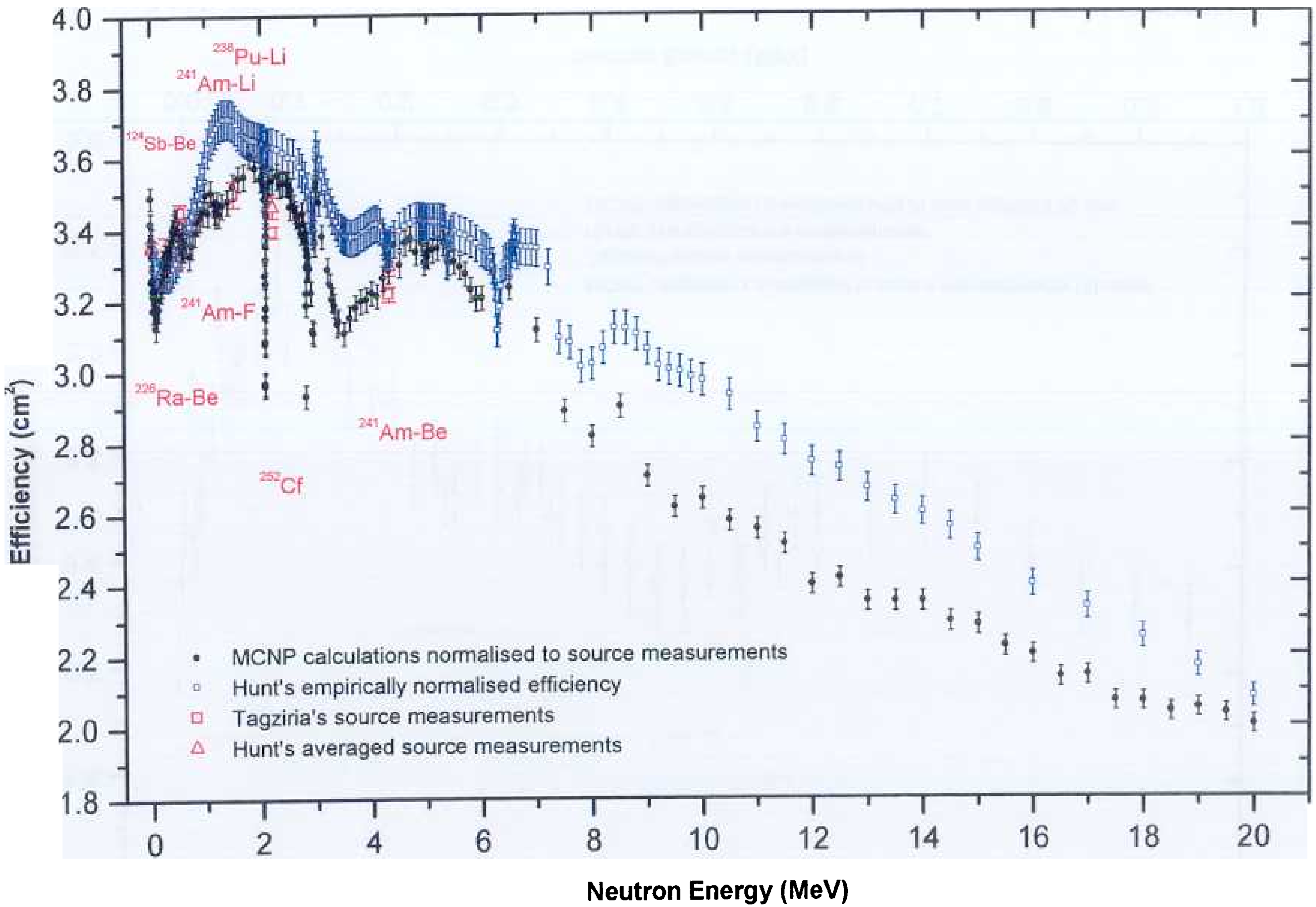

Figure 5.2 (c): Efficiency of the De Pangher Long Counter [0-20 MeV]

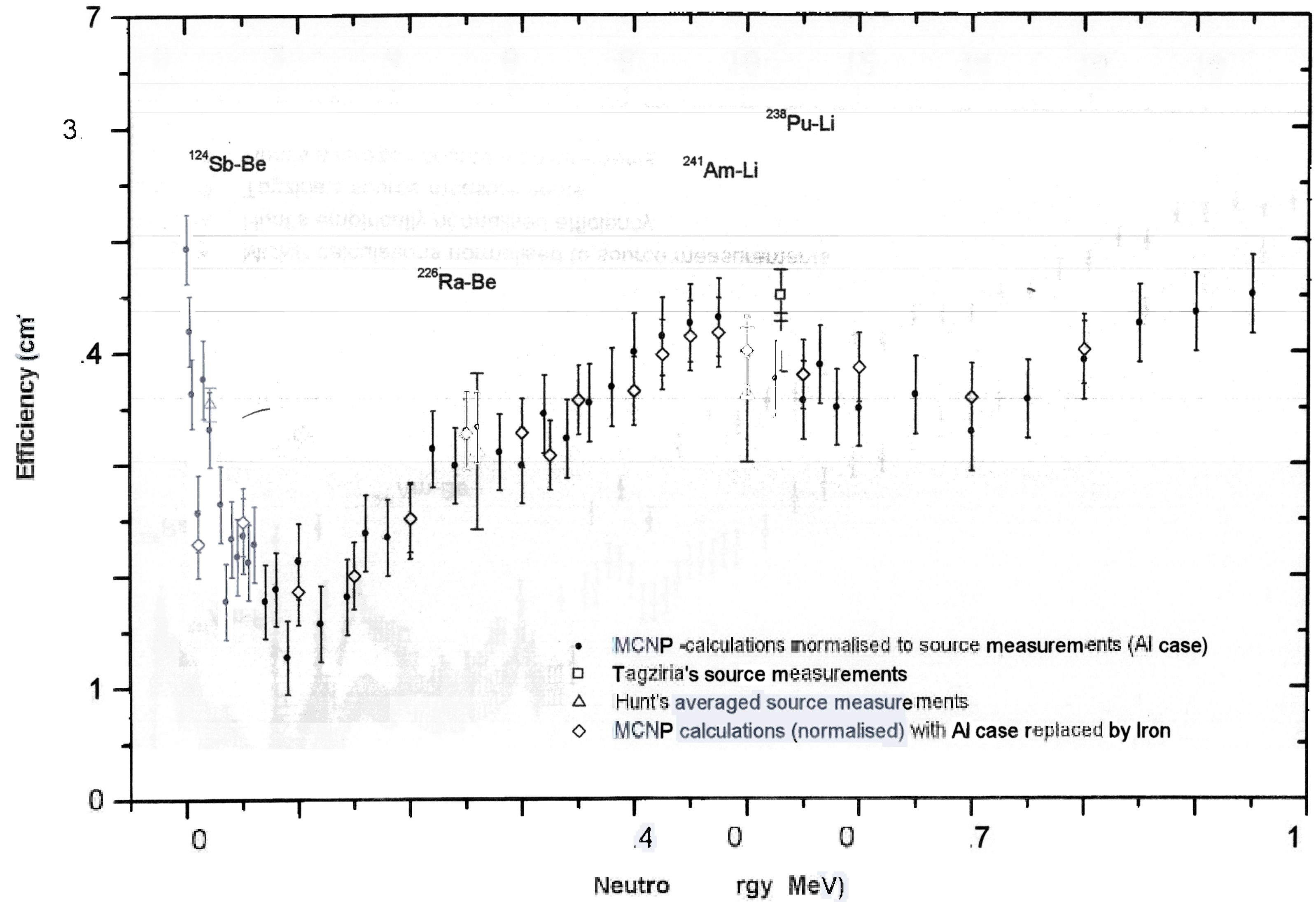

Fi (d): Efficie of the De her Long nter with the replaced by [0- M V]

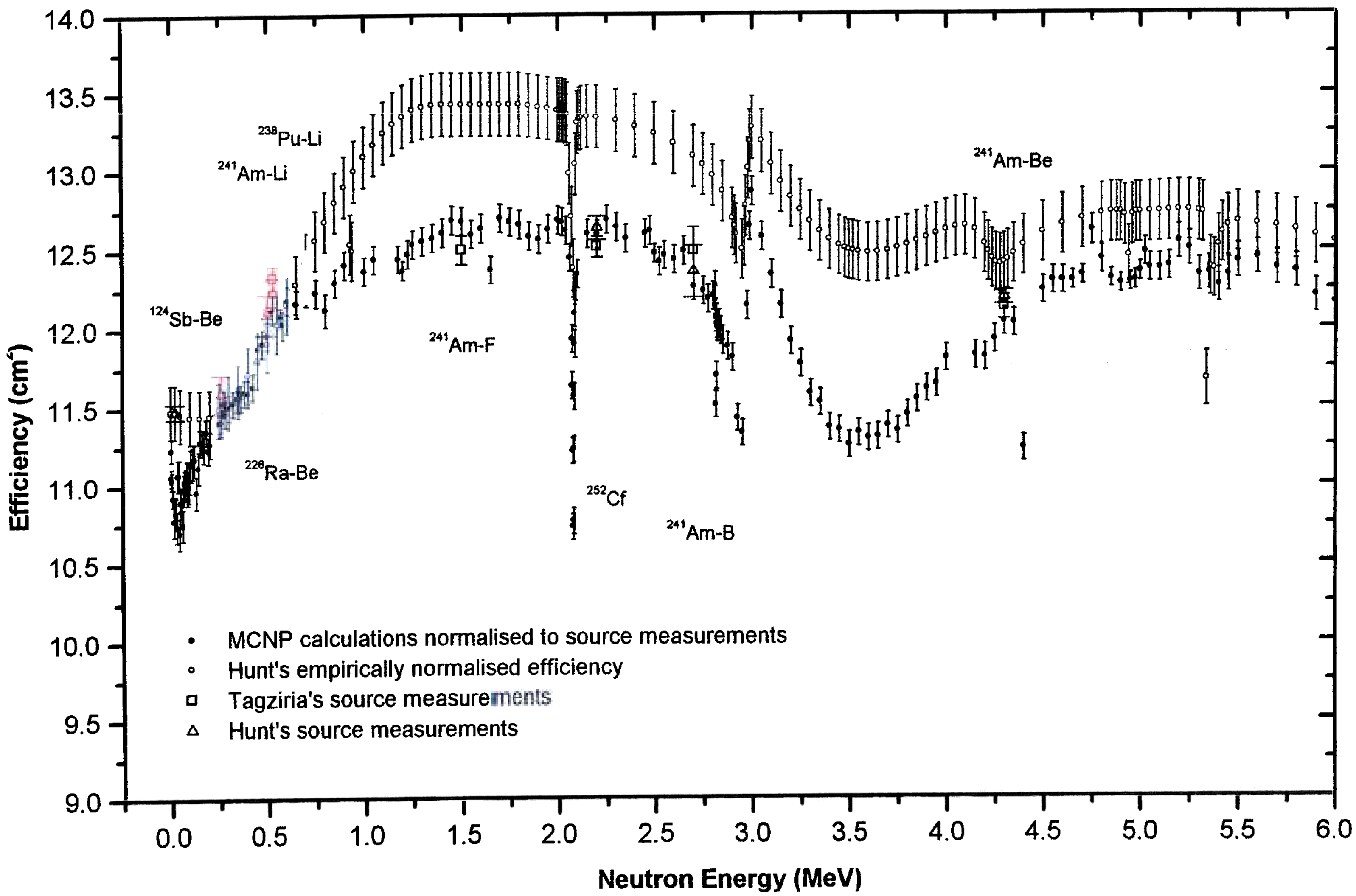

Figure 5.3(a): Efficiency of the NPL long counter [0-6 MeV]

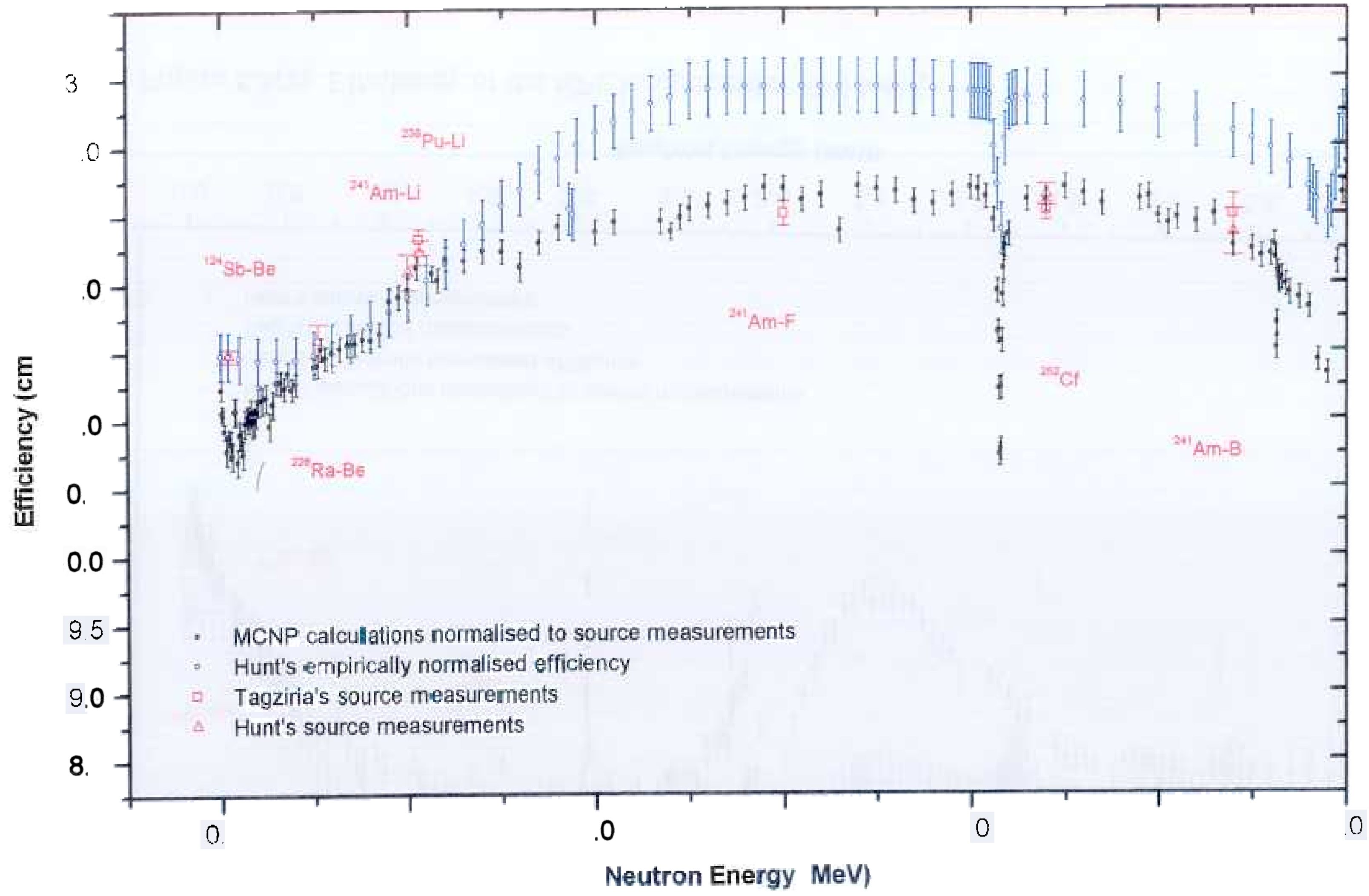

Fig re 5.3(b fficiency of th NPL long cou te 0-3 MeV]

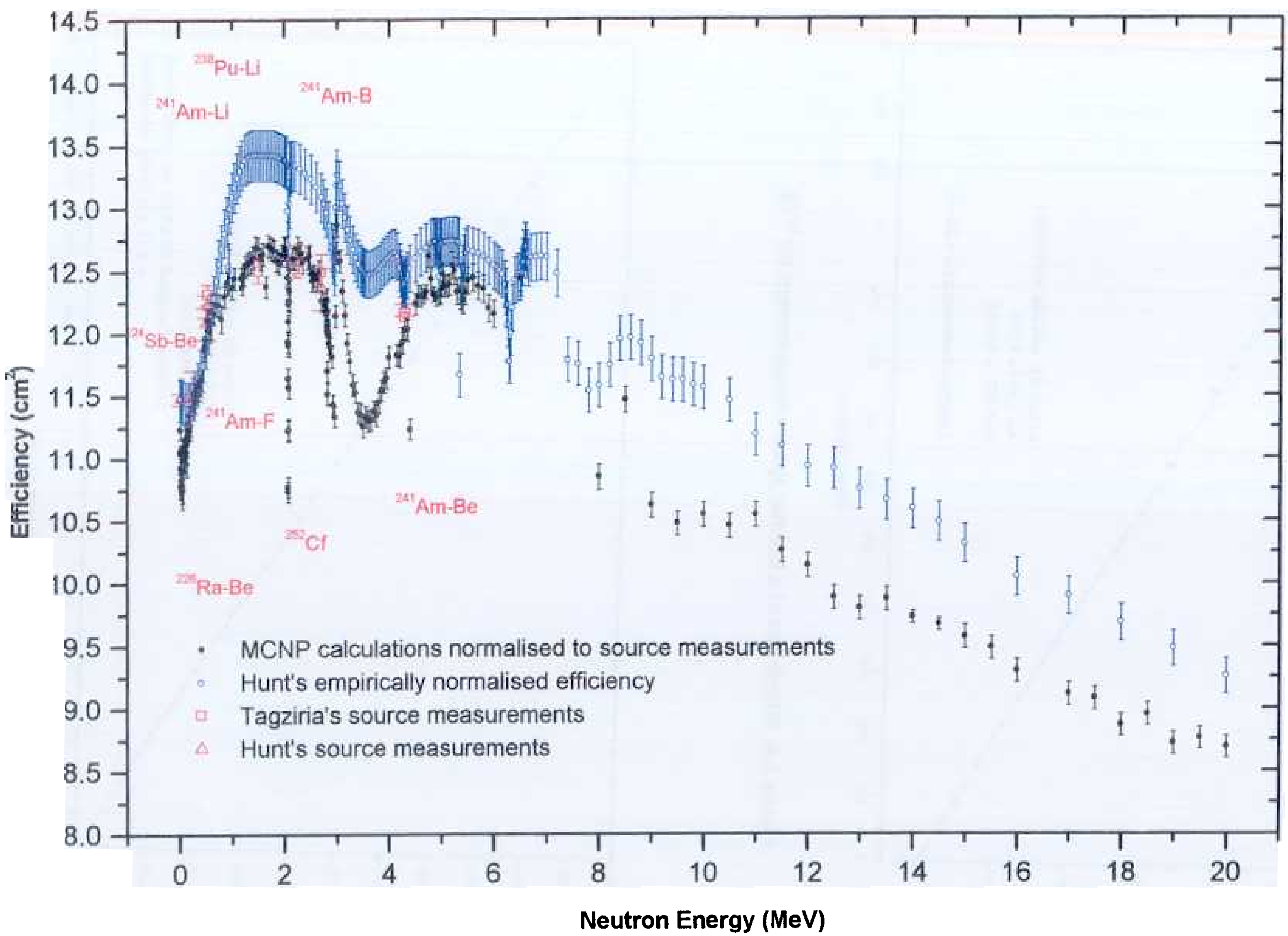

Figure 5.3(c): Efficiency of the NPL long counter [0-20 MeV]

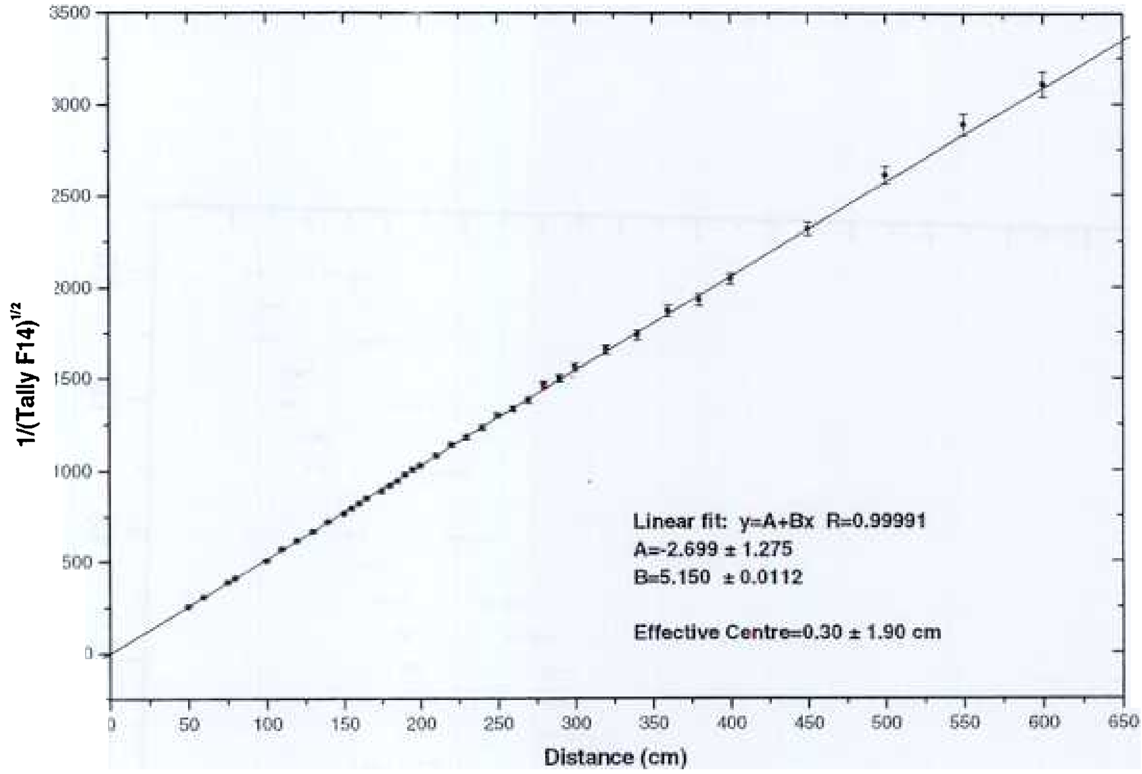

Figure 5.4: Simulation of a Bonner sphere measurement for ^{252}Cf

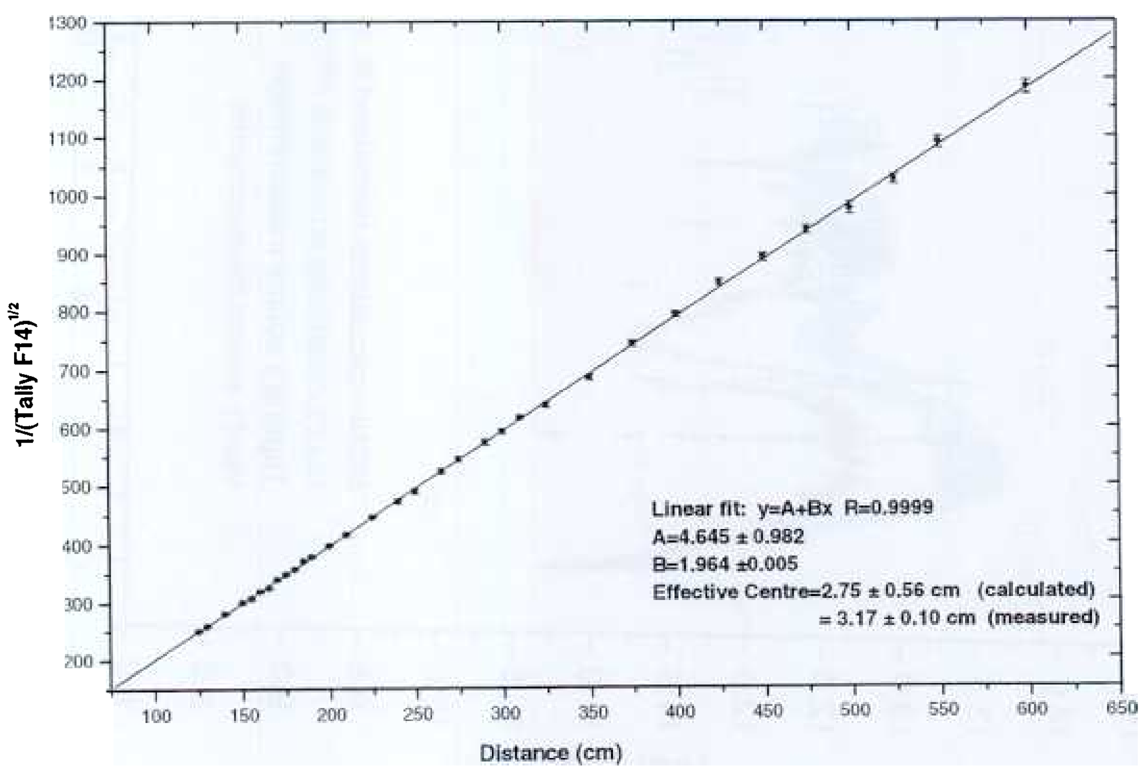

Figure 5.5 : Simulation of the De Pangher long counter measurement for ^{252}Cf

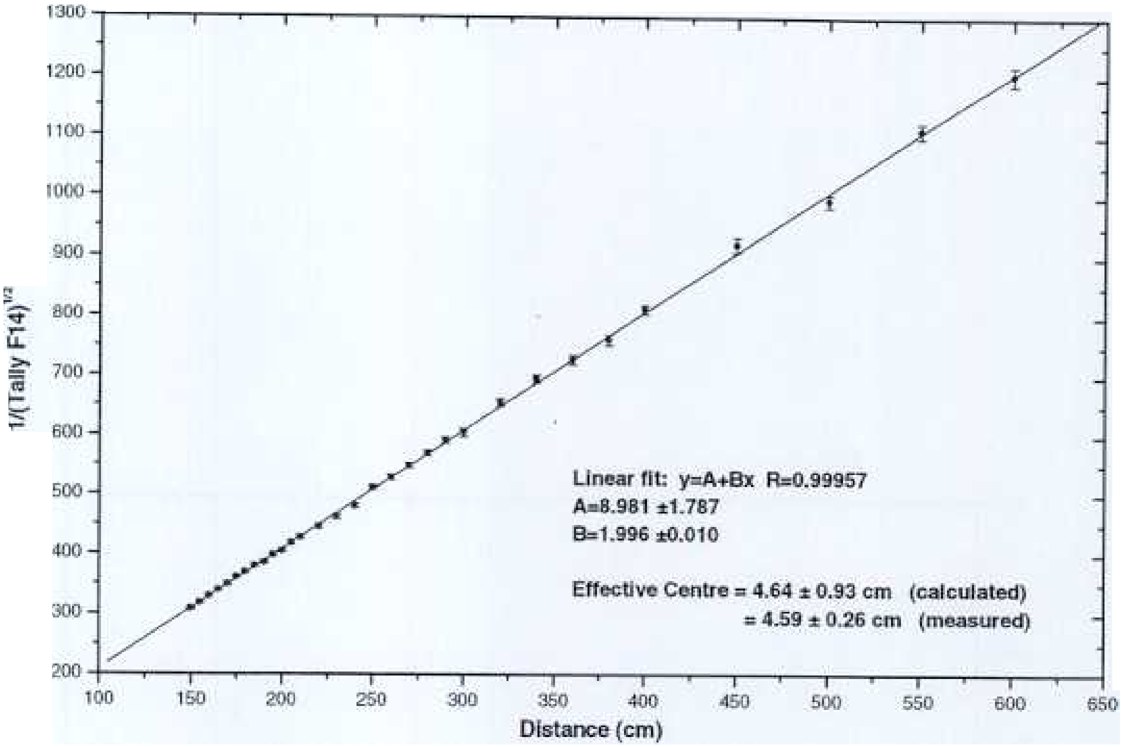

Figure 5.6 : Simulation of the De Pangher long counter measurement for ^{241}Am-Be

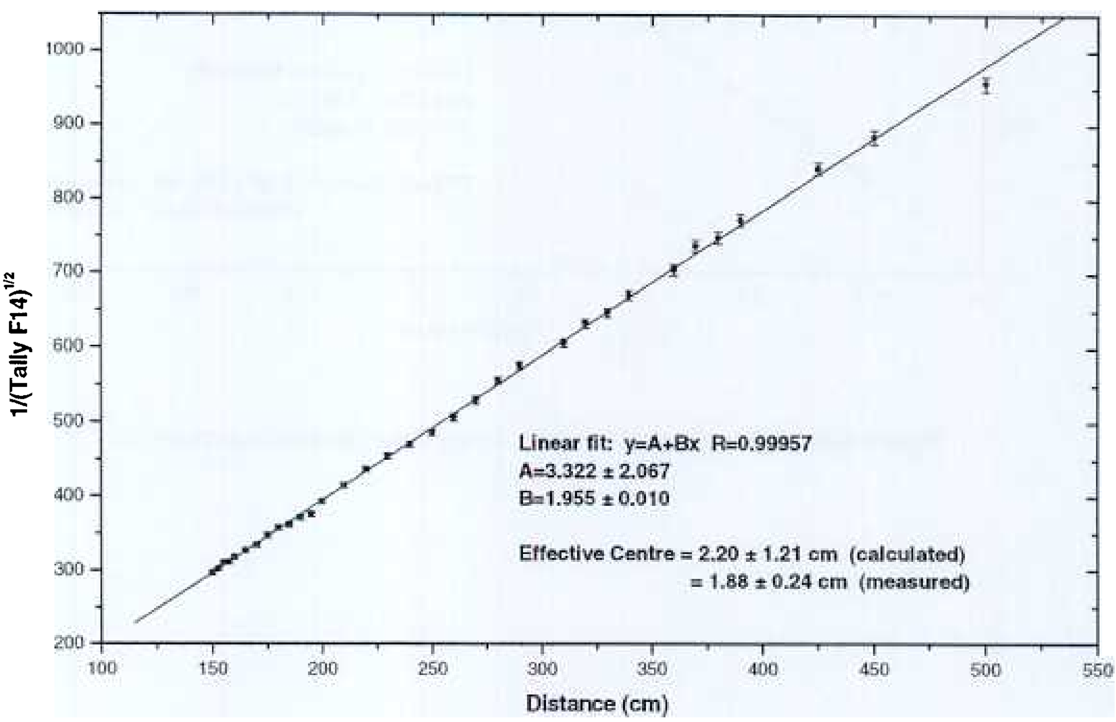

Figure 5.7 : Simulation of the De Pangher long counter measurement for 565 keV

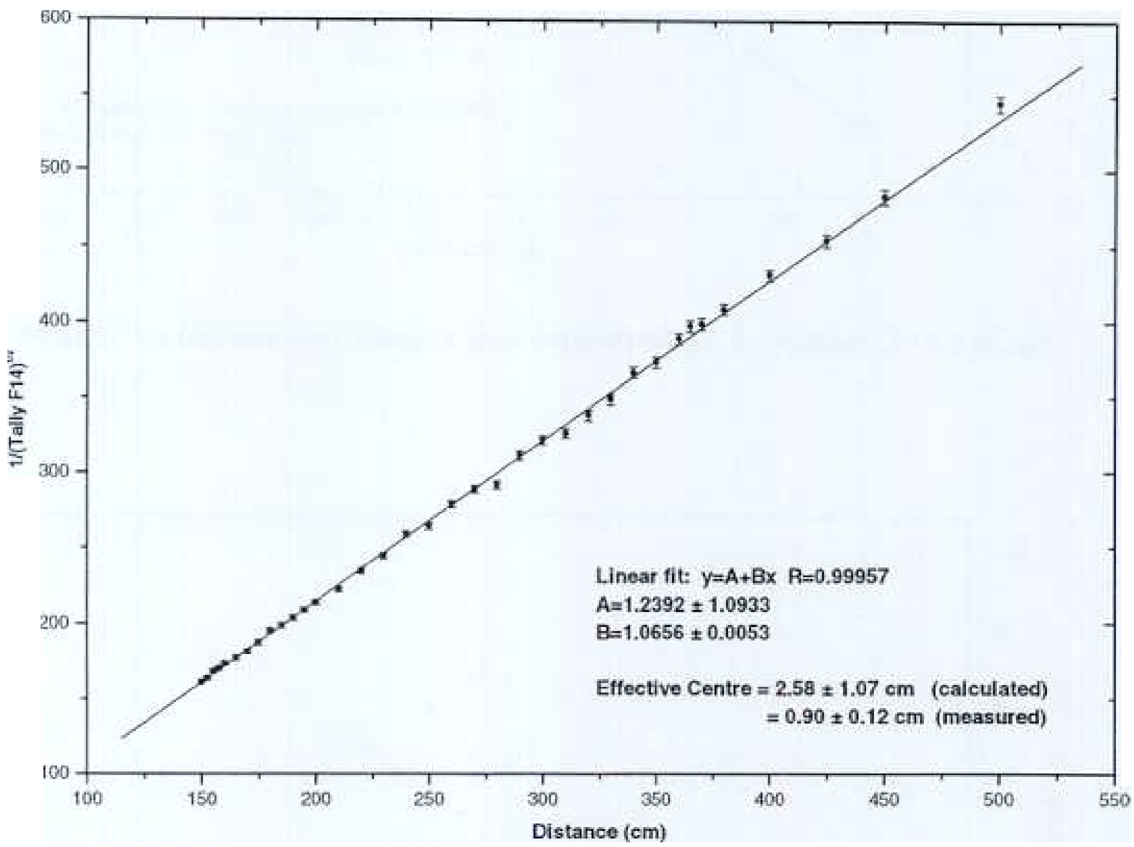

Figure 5.8 : Simulation of the NPL Long Counter measurement for ^{252}Cf

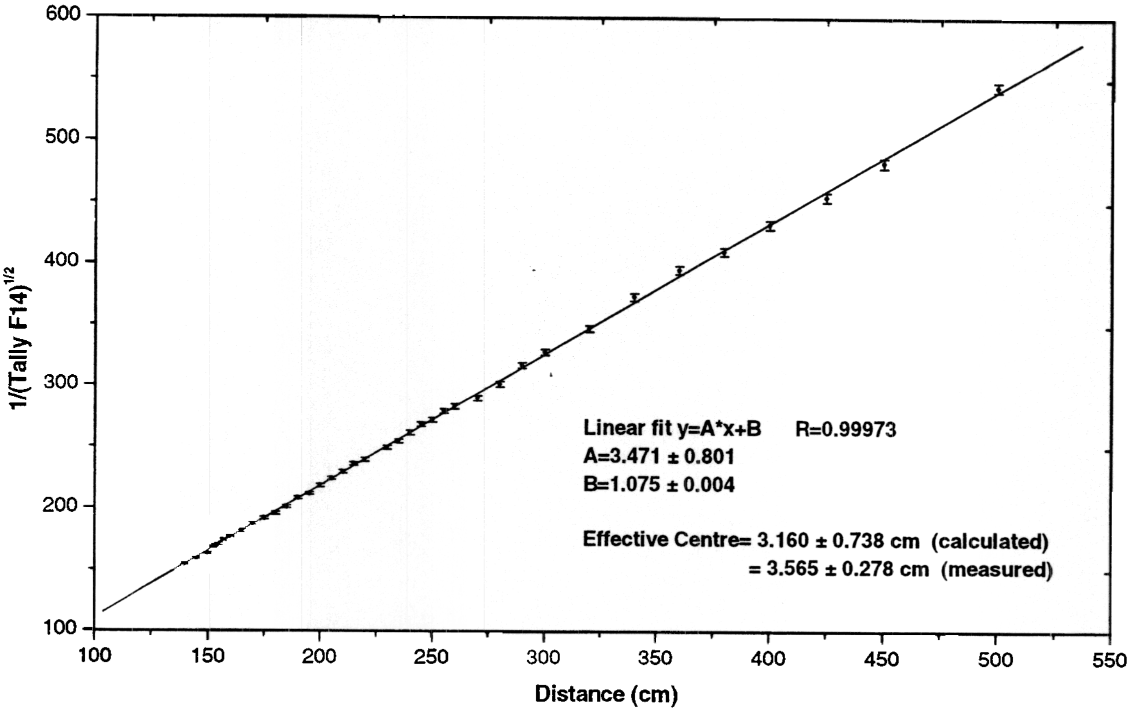

Figure 5.9 Simulation of NPL long counter measurement for ^{241}Am-Be

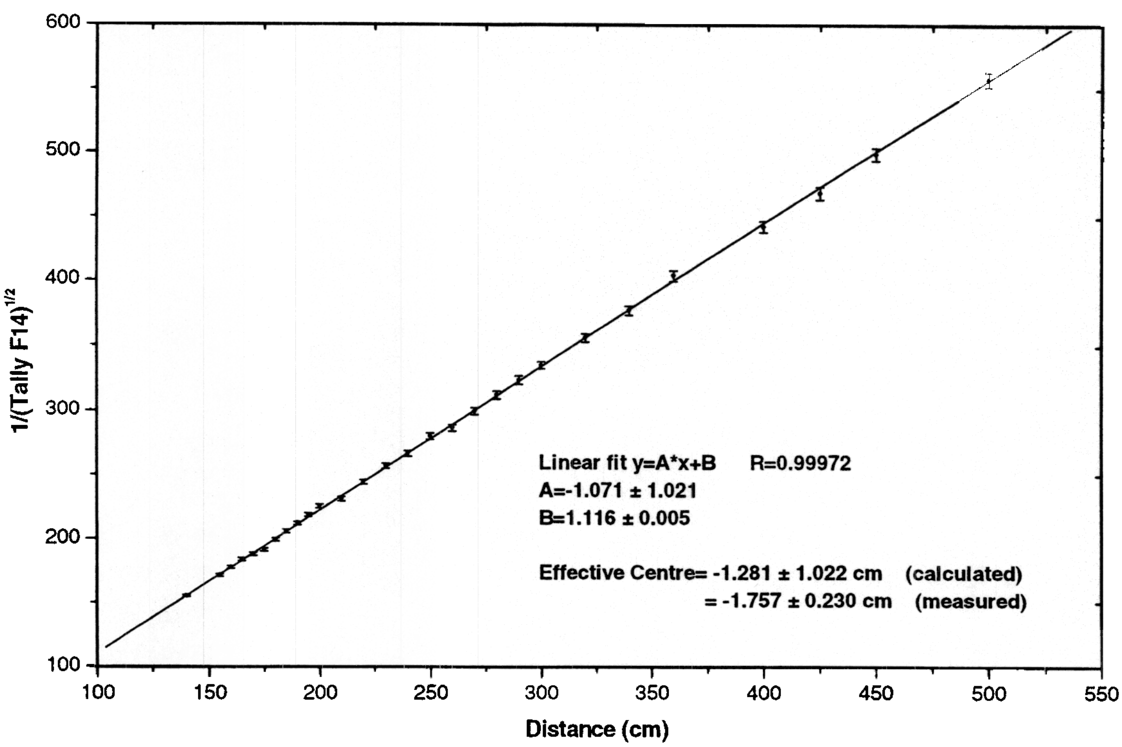

Figure 5.10 Simulation of NPL long counter measurement for 144 keV

Appendix A: PCINVFIT output file for the analysis of ^{252}Cf measurement with the De Pangher.

```
*****************************************************************************************************************
Run date:  05/03/1997                    Run time: 10:35:22
Output from program                      PCINVFIT
Input control parameters:                INT =  1   INTCENT =  0   INTSCH =  2
NUMBER OF MEASUREMENTS  :                43
NEUTRON COUNTER DEAD TIME                10.0000 MICROSECONDS
OUTSCATTER (AIR-ATTEN) FACTOR            ( 1055.0  E-7 ) CM-1.
*****************************************************************************************************************
```

DISTANCE (CMS)	DIRECT COUNTS	TIME (SECS)	DEAD-TIME CORRECTED CTS/SEC.	INSCATTER COUNTS	TIME (SECS)	DEAD-TIME CORRECTED CTS/SEC.	DIRECT-INSCATTER CTS/SEC.	OUTSCATTER CORRECTED CTS/SEC.	ERROR CTS/SEC.	1/(COR.)2	WEIGHT.
115.9	212607.	140.	1542.0	14856.	200.	74.3	1467.7	1485.8	3.4	.025943	.1108D+10
120.9	169117.	120.	1429.5	25362.	360.	70.5	1359.0	1376.4	3.5	.026954	.8281D+09
125.9	182226.	140.	1318.8	29593.	440.	67.3	1251.5	1268.2	3.2	.028080	.8193D+09
130.9	145401.	120.	1226.5	13121.	200.	65.6	1160.9	1177.0	3.3	.029148	.5944D+09
135.9	157896.	140.	1140.7	12761.	200.	63.8	1076.8	1092.4	3.0	.030256	.5919D+09
140.9	126285.	120.	1063.6	14971.	240.	62.4	1001.1	1016.1	3.1	.031371	.4420D+09
145.9	237353.	240.	998.8	12173.	200.	60.9	937.9	952.5	2.2	.032402	.7435D+09
150.9	74294.	80.	937.4	14638.	240.	61.0	876.4	890.4	3.5	.033512	.2264D+09
155.9	87263.	100.	880.3	14260.	240.	59.5	820.9	834.5	3.1	.034617	.2464D+09
165.9	77631.	100.	782.4	16378.	280.	58.5	723.9	736.6	2.9	.036845	.1907D+09
175.9	69746.	100.	702.4	22238.	400.	55.6	646.7	658.8	2.7	.038959	.1528D+09
185.9	63204.	100.	636.1	19543.	360.	54.3	581.7	593.3	2.6	.041056	.1226D+09
195.9	57189.	100.	575.2	16578.	320.	51.8	523.3	534.3	2.5	.043263	.9843D+08
205.9	52063.	100.	523.4	16160.	320.	50.5	472.8	483.2	2.4	.045492	.7974D+08
215.9	47806.	100.	480.4	15577.	320.	48.7	431.7	441.6	2.3	.047587	.6610D+08
225.9	43645.	100.	438.4	15252.	320.	47.7	390.7	400.1	2.2	.049994	.5366D+08
235.9	40710.	100.	408.8	18573.	400.	46.5	362.3	371.4	2.1	.051887	.4621D+08
245.9	37822.	100.	379.7	21312.	480.	44.4	335.2	344.0	2.0	.053913	.3962D+08
255.9	56054.	160.	351.6	21060.	480.	43.9	307.7	316.1	1.6	.056246	.5212D+08
265.9	117130.	360.	326.4	13809.	320.	43.2	283.3	291.3	1.1	.058590	.8949D+08
275.9	97731.	320.	306.3	13557.	320.	42.4	264.0	271.8	1.1	.060661	.6931D+08
285.9	114532.	400.	287.2	13477.	320.	42.1	245.0	252.5	1.0	.062929	.7120D+08
295.9	86287.	320.	270.4	13012.	320.	40.7	229.7	237.0	1.0	.064960	.5133D+08
305.9	80646.	320.	252.7	12758.	320.	39.9	212.8	219.7	1.0	.067458	.4343D+08
315.9	95826.	400.	240.1	15709.	400.	39.3	200.9	207.7	.9	.069394	.4787D+08
325.9	90337.	400.	226.4	12201.	320.	38.1	188.2	194.8	.9	.071649	.4021D+08
335.9	107460.	500.	215.4	15158.	400.	37.9	177.5	183.9	.8	.073746	.4400D+08
345.9	81823.	400.	205.0	17669.	480.	36.8	168.2	174.4	.8	.075722	.3342D+08
355.9	96539.	500.	193.5	17415.	480.	36.3	157.2	163.2	.7	.078285	.3479D+08
365.9	73695.	400.	184.6	17867.	500.	35.7	148.8	154.7	.8	.080403	.2568D+08
375.9	105357.	600.	175.9	38831.	1100.	35.3	140.6	146.3	.6	.082682	.3550D+08
385.9	67104.	400.	168.0	24416.	700.	34.9	133.1	138.7	.7	.084916	.2089D+08
395.9	128716.	800.	161.2	13492.	400.	33.7	127.4	132.8	.6	.086761	.3015D+08
405.9	61692.	400.	154.5	16810.	500.	33.6	120.8	126.1	.7	.089043	.1622D+08
415.9	118882.	800.	148.8	16580.	500.	33.2	115.7	120.8	.5	.090969	.2559D+08
425.9	67691.	480.	141.2	16315.	500.	32.6	108.6	113.6	.6	.093835	.1488D+08
435.9	136565.	1000.	136.8	15955.	500.	31.9	104.8	109.8	.5	.095448	.2403D+08
445.9	84287.	640.	131.9	16034.	500.	32.1	99.8	104.6	.5	.097776	.1540D+08
455.9	102466.	800.	128.2	37496.	1200.	31.3	97.0	101.8	.5	.099127	.2053D+08
465.9	122455.	1000.	122.6	37009.	1200.	30.9	91.8	96.4	.4	.101862	.2186D+08
475.9	567246.	4800.	118.3	146475.	4800.	30.5	87.8	92.3	.2	.104081	.9169D+08
485.9	159973.	1400.	114.4	36668.	1200.	30.6	83.8	88.2	.3	.106455	.2312D+08
495.9	5737192.	52000.	110.5	1558173.	52000.	30.0	80.5	84.8	.1	.108592	.8128D+09

****

LEAST SQUARES FIT   NORMAL NPL PROCEEDURE CALCULATING EFFECTIVE CENTRE

DISTANCE (CMS)	1/(COR.)$\frac{1}{2}$	WEIGHT.	CALCULATED FIT	DIFFERENCE	PERCENT DIFFERRENCE	W(I)*(DIFF*DIFF)
115.90	.025943	.1108D+10	.025903	.000041	.156471	1.82550
120.90	.026954	.8281D+09	.026990	-.000036	-.134123	1.08228
125.90	.028080	.8193D+09	.028078	.000002	.008204	.00435
130.90	.029148	.5944D+09	.029166	-.000018	-.061953	.19382
135.90	.030256	.5919D+09	.030254	.000002	.007526	.00307
140.90	.031371	.4420D+09	.031341	.000029	.093372	.37920
145.90	.032402	.7435D+09	.032429	-.000027	-.084138	.55259
150.90	.033512	.2264D+09	.033517	-.000004	-.013266	.00447
155.90	.034617	.2464D+09	.034604	.000013	.037348	.04118
165.90	.036845	.1907D+09	.036780	.000065	.175546	.79794
175.90	.038959	.1528D+09	.038955	.000004	.009554	.00212
185.90	.041056	.1226D+09	.041131	-.000075	-.182338	.68692
195.90	.043263	.9843D+08	.043306	-.000043	-.099496	.18237
205.90	.045492	.7974D+08	.045482	.000010	.021988	.00798
215.90	.047587	.6610D+08	.047657	-.000070	-.147662	.32639
225.90	.049994	.5366D+08	.049832	.000161	.322633	1.39611
235.90	.051887	.4621D+08	.052008	-.000121	-.233575	.67874
245.90	.053913	.3962D+08	.054183	-.000271	-.501829	2.90010
255.90	.056246	.5212D+08	.056359	-.000113	-.200380	.66204
265.90	.058590	.8949D+08	.058534	.000056	.095138	.27806
275.90	.060661	.6931D+08	.060710	-.000049	-.080110	.16368
285.90	.062929	.7120D+08	.062885	.000044	.069911	.13781
295.90	.064960	.5133D+08	.065060	-.000101	-.155092	.52098
305.90	.067458	.4343D+08	.067236	.000223	.329960	2.15180
315.90	.069394	.4787D+08	.069411	-.000017	-.024243	.01355
325.90	.071649	.4021D+08	.071587	.000063	.087284	.15727
335.90	.073746	.4400D+08	.073762	-.000016	-.021923	.01150
345.90	.075722	.3342D+08	.075938	-.000215	-.284253	1.54829
355.90	.078285	.3479D+08	.078113	.000172	.220033	1.03240
365.90	.080403	.2568D+08	.080288	.000114	.142320	.33619
375.90	.082682	.3550D+08	.082464	.000218	.263794	1.68867
385.90	.084916	.2089D+08	.084639	.000277	.325874	1.60000
395.90	.086761	.3015D+08	.086815	-.000054	-.062058	.08740
405.90	.089043	.1622D+08	.088990	.000053	.059802	.04600
415.90	.090969	.2559D+08	.091166	-.000196	-.215803	.98612
425.90	.093835	.1488D+08	.093341	.000494	.526628	3.63379
435.90	.095448	.2403D+08	.095516	-.000068	-.071367	.11150
445.90	.097776	.1540D+08	.097692	.000084	.086310	.10970
455.90	.099127	.2053D+08	.099867	-.000740	-.746820	11.24887
465.90	.101862	.2186D+08	.102043	-.000181	-.177305	.71304
475.90	.104081	.9169D+08	.104218	-.000137	-.131498	1.71743
485.90	.106455	.2312D+08	.106393	.000061	.057728	.08732
495.90	.108592	.8128D+09	.108569	.000023	.021559	.44549

****

****

NO. OF DEGREES OF FREEDOM = 41 CHISQ= 40.55405 ChISQ/DEG. OF FREEDOM = .98912

GRADIENT FROM LSQ FIT IS .217543D-03 AND ITS ERROR + OR - .887237D-07

INTERCEPT FROM LSQ FIT IS .689545D-03 AND ITS ERROR + OR - .207694D-04

EFFECTIVE CENTRE IS THUS (-3.1697 + OR - .0955)CMS.

****

LEAST SQUARES FIT NORMAL NPL PROCEEDURE CALCULATING EFFECTIVE CENTRE

NO. OF POINT	RANGE OF DISTANCES MIN(CMS.)	MAX(CMS.)	GRADIENT AND ITS ERROR.			INTERCEPT AND ITS ERROR,			EFFECTIVE CENTRE (CMS.)		
43	115.90	495.90	.217543D-03	+/-	.887237D-07	.689545D-03	+/-	.207694D-04	-3.1697	+/-	.0955
42	115.90	485.90	.217406D-03	+/-	.146009D-06	.709640D-03	+/-	.268376D-04	-3.2641	+/-	.1235
41	115.90	475.90	.217388D-03	+/-	.151289D-06	.712327D-03	+/-	.275458D-04	-3.2768	+/-	.1267
40	115.90	465.90	.217459D-03	+/-	.170062D-06	.701868D-03	+/-	.298046D-04	-3.2276	+/-	.1371
39	115.90	455.90	.217491D-03	+/-	.176352D-06	.697269D-03	+/-	.306232D-04	-3.2060	+/-	.1408
38	115.90	445.90	.217634D-03	+/-	.153348D-06	.676501D-03	+/-	.264051D-04	-3.1084	+/-	.1213
37	115.90	435.90	.217626D-03	+/-	.158669D-06	.677727D-03	+/-	.271546D-04	-3.1142	+/-	.1248
36	115.90	425.90	.217648D-03	+/-	.165580D-06	.674509D-03	+/-	.280765D-04	-3.0991	+/-	.1290
35	115.90	415.90	.217578D-03	+/-	.159926D-06	.684520D-03	+/-	.269682D-04	-3.1461	+/-	.1240
34	115.90	405.90	.217633D-03	+/-	.163498D-06	.676655D-03	+/-	.273188D-04	-3.1092	+/-	.1255
33	115.90	395.90	.217628D-03	+/-	.169543D-06	.677365D-03	+/-	.281707D-04	-3.1125	+/-	.1295
32	115.90	385.90	.217653D-03	+/-	.178229D-06	.673841D-03	+/-	.293188D-04	-3.0959	+/-	.1347
31	115.90	375.90	.217596D-03	+/-	.179868D-06	.681979D-03	+/-	.293912D-04	-3.1342	+/-	.1351
30	115.90	365.90	.217511D-03	+/-	.183046D-06	.693883D-03	+/-	.295857D-04	-3.1901	+/-	.1360
29	115.90	355.90	.217474D-03	+/-	.190159D-06	.699058D-03	+/-	.305030D-04	-3.2144	+/-	:1403
28	115.90	345.90	.217394D-03	+/-	.194291D-06	.710246D-03	+/-	.308601D-04	-3.2671	+/-	.1420
27	115.90	335.90	.217472D-03	+/-	.198218D-06	.699328D-03	+/-	.311995D-04	-3.2157	+/-	.1435
26	115.90	325.90	.217474D-03	+/-	.213177D-06	.699132D-03	+/-	.331725D-04	-3.2148	+/-	.1526
25	115.90	315.90	.217431D-03	+/-	.226540D-06	.705041D-03	+/-	.349011D-04	-3.2426	+/-	.1606
24	115.90	305.90	.217429D-03	+/-	.245270D-06	.705333D-03	+/-	.373597D-04	-3.2440	+/-	.1719
23	115.90	295.90	.217262D-03	+/-	.237857D-06	.728040D-03	+/-	.358770D-04	-3.3510	+/-	.1652
22	115.90	285.90	.217311D-03	+/-	.257122D-06	.721385D-03	+/-	.383594D-04	-3.3196	+/-	.1766
21	115.90	275.90	.217205D-03	+/-	.281478D-06	.735729D-03	+/-	.413887D-04	-3.3872	+/-	.1906
20	115.90	265.90	.217208D-03	+/-	.316393D-06	.735378D-03	+/-	.459019D-04	-3.3856	+/-	.2114
19	115.90	255.90	.216979D-03	+/-	.350205D-06	.766063D-03	+/-	.499758D-04	-3.5306	+/-	.2304
18	115.90	245.90	.217045D-03	+/-	.387962D-06	.757258D-03	+/-	.548659D-04	-3.4889	+/-	.2529
17	115.90	235.90	.217293D-03	+/-	.377760D-06	.724255D-03	+/-	.530880D-04	-3.3331	+/-	.2444
16	115.90	225.90	.217428D-03	+/-	.403361D-06	.706386D-03	+/-	.563105D-04	-3.2488	+/-	.2591
15	115.90	215.90	.217142D-03	+/-	.390341D-06	.744081D-03	+/-	.541166D-04	-3.4267	+/-	.2493
14	115.90	205.90	.217226D-03	+/-	.435172D-06	.733147D-03	+/-	.598751D-04	-3.3751	+/-	.2757
13	115.90	195.90	.217138D-03	+/-	.492069D-06	.744595D-03	+/-	.671585D-04	-3.4291	+/-	.3094
12	115.90	185.90	.217206D-03	+/-	.567870D-06	.735716D-03	+/-	.768344D-04	-3.3872	+/-	.3539
11	115.90	175.90	.217489D-03	+/-	.635006D-06	.699208D-03	+/-	.851279D-04	-3.2149	+/-	.3915
10	115.90	165.90	.217468D-03	+/-	.759581D-06	.702002D-03	+/-	.100854D-03	-3.2281	+/-	.4639
9	115.90	155.90	.216944D-03	+/-	.810929D-06	.768381D-03	+/-	.106638D-03	-3.5418	+/-	.4917
8	115.90	150.90	.216677D-03	+/-	.944670D-06	.801693D-03	+/-	.123060D-03	-3.6999	+/-	.5682
7	115.90	145.90	.216552D-03	+/-	.111962D-05	.817186D-03	+/-	.144745D-03	-3.7736	+/-	.6687
6	115.90	140.90	.217059D-03	+/-	.165006D-05	.755115D-03	+/-	.208312D-03	-3.4788	+/-	.9601
5	115.90	135.90	.215863D-03	+/-	.208318D-05	.900191D-03	+/-	.259343D-03	-4.1702	+/-	1.2021

****

****

LEAST SQUARES FIT   NORMAL NPL PROCEEDURE CALCULATING EFFECTIVE CENTRE

NO. OF POINT	RANGE OF DISTANCES MIN(CMS.)	MAX(CMS.)	GRADIENT AND ITS ERROR.		INTERCEPT AND ITS ERROR,		EFFECTIVE CENTRE (CMS.)	
43	115.90	495.90	.217543D-03 +/-	.887237D-07	.689545D-03 +/-	.207694D-04	-3.1697 +/-	.0955
42	120.90	495.90	.217579D-03 +/-	.904966D-07	.675413D-03 +/-	.223977D-04	-3.1042 +/-	.1029
41	125.90	495.90	.217559D-03 +/-	.939588D-07	.683523D-03 +/-	.243960D-04	-3.1418 +/-	.1121
40	130.90	495.90	.217565D-03 +/-	.993182D-07	.681200D-03 +/-	.272298D-04	-3.1310 +/-	.1252
39	135.90	495.90	.217555D-03 +/-	.104597D-06	.685196D-03 +/-	.300015D-04	-3.1495 +/-	.1379
38	140.90	495.90	.217559D-03 +/-	.111585D-06	.683267D-03 +/-	.336847D-04	-3.1406 +/-	.1548
37	145.90	495.90	.217587D-03 +/-	.117981D-06	.671690D-03 +/-	.371915D-04	-3.0870 +/-	.1709
36	150.90	495.90	.217553D-03 +/-	.135573D-06	.686286D-03 +/-	.466168D-04	-3.1546 +/-	.2143
35	155.90	495.90	.217551D-03 +/-	.146087D-06	.687191D-03 +/-	.518170D-04	-3.1588 +/-	.2382
34	165.90	495.90	.217565D-03 +/-	.161175D-06	.680746D-03 +/-	.593093D-04	-3.1289 +/-	.2726
33	175.90	495.90	.217634D-03 +/-	.174679D-06	.650636D-03 +/-	.662706D-04	-2.9896 +/-	.3045
32	185.90	495.90	.217659D-03 +/-	.191763D-06	.639642D-03 +/-	.746566D-04	-2.9387 +/-	.3430
31	195.90	495.90	.217618D-03 +/-	.209230D-06	.657840D-03 +/-	.832391D-04	-3.0229 +/-	.3825
30	205.90	495.90	.217597D-03 +/-	.227954D-06	.667288D-03 +/-	.923299D-04	-3.0666 +/-	.4243
29	215.90	495.90	.217613D-03 +/-	.247069D-06	.660356D-03 +/-	.101570D-03	-3.0346 +/-	.4668
28	225.90	495.90	.217575D-03 +/-	.265592D-06	.677364D-03 +/-	.110555D-03	-3.1132 +/-	.5081
27	235.90	495.90	.217671D-03 +/-	.277445D-06	.633200D-03 +/-	.116670D-03	-2.9090 +/-	.5360
26	245.90	495.90	.217621D-03 +/-	.293705D-06	.656426D-03 +/-	.124593D-03	-3.0164 +/-	.5725
25	255.90	495.90	.217500D-03 +/-	.297424D-06	.712693D-03 +/-	.127112D-03	-3.2767 +/-	.5844
24	265.90	495.90	.217417D-03 +/-	.314959D-06	.751690D-03 +/-	.135921D-03	-3.4574 +/-	.6252
23	275.90	495.90	.217454D-03 +/-	.354974D-06	.734152D-03 +/-	.155802D-03	-3.3761 +/-	.7165
22	285.90	495.90	.217368D-03 +/-	.394682D-06	.775025D-03 +/-	.175565D-03	-3.5655 +/-	.8077
21	295.90	495.90	.217381D-03 +/-	.450664D-06	.768736D-03 +/-	.203290D-03	-3.5363 +/-	.9352
20	305.90	495.90	.217208D-03 +/-	.496339D-06	.851847D-03 +/-	.226184D-03	-3.9218 +/-	1.0414
19	315.90	495.90	.217414D-03 +/-	.541088D-06	.752487D-03 +/-	.248701D-03	-3.4611 +/-	1.1439
18	325.90	495.90	.217349D-03 +/-	.618225D-06	.784097D-03 +/-	.286840D-03	-3.6076 +/-	1.3198
17	335.90	495.90	.217400D-03 +/-	.705009D-06	.759327D-03 +/-	.329677D-03	-3.4928 +/-	1.5165
16	345.90	495.90	.217315D-03 +/-	.826417D-06	.800419D-03 +/-	.389737D-03	-3.6832 +/-	1.7935
15	355.90	495.90	.216819D-03 +/-	.906652D-06	.104168D-02 +/-	.430288D-03	-4.8044 +/-	1.9846
14	365.90	495.90	.217019D-03 +/-	.106956D-05	.944438D-03 +/-	.510870D-03	-4.3519 +/-	2.3541
13	375.90	495.90	.217132D-03 +/-	.124371D-05	.889048D-03 +/-	.596780D-03	-4.0945 +/-	2.7486
12	385.90	495.90	.217839D-03 +/-	.149912D-05	.542958D-03 +/-	.723740D-03	-2.4925 +/-	3.3224
11	395.90	495.90	.218711D-03 +/-	.166662D-05	.115167D-03 +/-	.807367D-03	-.5266 +/-	3.6915
10	405.90	495.90	.219036D-03 +/-	.215084D-05	-.446505D-04 +/-	.104682D-02	.2038 +/-	4.7792
9	415.90	495.90	.219669D-03 +/-	.255151D-05	-.355998D-03 +/-	.124475D-02	1.6206 +/-	5.6665
8	425.90	495.90	.219398D-03 +/-	.342599D-05	-.222513D-03 +/-	.167705D-02	1.0142 +/-	7.6439
7	435.90	495.90	.222606D-03 +/-	.323117D-05	-.180391D-02 +/-	.158452D-02	8.1036 +/-	7.1190
6	445.90	495.90	.225231D-03 +/-	.414872D-05	-.309954D-02 +/-	.203967D-02	13.7616 +/-	9.0595
5	455.90	495.90	.229277D-03 +/-	.372088D-05	-.509826D-02 +/-	.183190D-02	22.2363 +/-	7.9981

****

Appendix B

Compendium of efficiency and effective centre source measurements for the NPL long counter by Tagziria (HT) and Hunt (JH)

Source	Mean Energy	Measurement	Efficiency	Error (1S)	Effective Centre (cm)	Error (1S)
^{252}Cf	2.2	JH				
		18/12/72	12.632	0.035	3.300	0.280
		8/4/81	12.739	0.040	3.560	0.260
		9/1/74	12.593	0.033	3.730	0.270
		11/11/83	12.568	0.034	3.380	0.300
		RS5 76 (reference 6)	12.730	0.080	3.460	0.270
		Average	**12.652**	**0.036**	**3.486**	**0.276**
		Std. Deviation	**0.078**		**0.192**	
		HT	12.512	0.065	0.902	0.116
		Average(JH&HT)	**12.582**			
		Std. Deviation	**0.099**			
^{226}Ra-Be	0.26	JH/1/6/1973	11.580	0.120	1.220	1.010
		RS5 76	11.800	0.160		
		Average:	**11.690**			
		Std. Deviation	**0.156**			
^{241}Am-Li	0.53	JH/5/1/1973	12.080	0.130	-0.420	1.040
		RS5	12.270	0.140		
		Average:	**12.175**			
		Std. Deviation	**0.134**			
^{241}Am-Be	4.3	JH/11/1/1982 (13pts)	12.215	0.082	5.220	0.590
		RS5	12.150	0.100	6.220	0.530
		Average:	**12.183**			
		Std. Deviation	**0.046**			
		HT	12.121	0.075	3.565	0.278
		Average (HT&JH):	**12.152**			
		Std. Deviation	**0.022**			
^{241}Am-B	2.7	**JH**/11/82 (13pts)	12.353	0.167	3.890	1.180
		HT	12.312	0.078	2.660	0.317
		Average(JH&HT)	**12.333**			
		Std. Deviation	**0.029**			
^{124}Sb-Be	0.021	JH/13/2/78	11.473	0.048	-0.720	0.440
^{238}Pu-Li	0.5	JH/5/2/86(21pts)	12.220	0.090	-0.850	0.660
		HT	12.486	0.147	3.634	1.310
		Average(JH&HT)	**12.353**			
		Std. Deviation	**0.188**			
^{241}Am-F	1.46	HT	12.494	0.091	0.495	0.670